

## **CHAPTER SIX**

# **Oscillating-Body Wave-Energy Converters**

This chapter starts with a consideration of wave absorption as a destructive interference between an incident wave and a wave radiated by an immersed oscillating-body wave-energy converter (WEC). Then, various WECs are classified according to size and orientation with respect to wavelength and propagation direction, respectively, of the incident wave. Next, for a given incident sinusoidal wave, mathematical expressions are derived for the wave power which is absorbed by a single-mode oscillating WEC body, as a function of its velocity amplitude and phase. A particular subject of interest is the optimum motion for maximising the power absorbed from the sea wave, as is also control methods to obtain optimum WEC oscillation.

Concerning the WEC's size, only its maximum horizontal extension has been considered thus far. However, for a particular WEC discussed in Section 6.4, not only the WEC body's volume but also its geometrical shape are considered.

### **6.1 Wave Absorption as Wave Interference**

Absorbing wave energy means that energy has to be removed from the waves. Hence, there must be a cancellation or reduction of waves which are passing a WEC or are being reflected from it. Such a cancellation or reduction of waves can be realised by the oscillating WEC, provided it generates waves which oppose (are in counterphase with) the passing and/or reflected waves. In other words, the generated wave has to interfere destructively with the other waves.

Within classical theories for microphones or receiving antennae, it is a well-known point of view that to absorb an acoustic or electromagnetic wave means to radiate a wave that interferes destructively with the incident wave. Concerning absorption of an incoming ocean wave by means of an immersed oscillating body, Budal may have been the first to explain such a view, which he stated as follows: 'a secondary, ring-shaped, outgoing wave is generated, which interferes with the incoming wave in such a way that the resulting transmitted wave carries

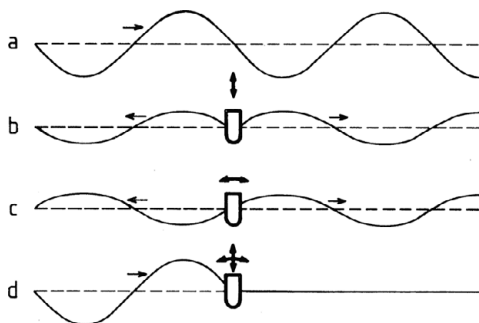


Figure 6.1: To absorb waves means to generate waves. Curve *a* represents an undisturbed incident wave moving from left to right on water in a narrow wave channel. Curve *b* illustrates symmetric wave generation (on otherwise calm water) by a floating symmetric body oscillating in the heave mode (up and down). Curve *c* illustrates antisymmetric wave generation by the same body oscillating in the surge and/or pitch mode. Curve *d*, which represents the superposition (sum) of the three waves, illustrates complete absorption of the incident wave energy.

with it less energy than the incoming wave does' [70]. To radiate an outgoing wave, the WEC needs to displace water, in an oscillatory manner.

A simple example to illustrate this fact is shown in Figure 6.1. Here, a floating symmetric body is immersed in a narrow flume (water between two parallel glass walls). Complete wave-energy absorption is possible, theoretically, provided the body is simultaneously performing optimal oscillation in the vertical direction as well as in the horizontal direction. Because power is proportional to amplitude squared, the waves shown by curves *a*, *b* and *c* have amplitudes in ratios 2:1:1, but powers in ratios 4:1:1, respectively. Thus, if the body oscillates only in the vertical direction or only in the horizontal direction, then one-half of the incident wave energy is received by the oscillating body. The remaining half is separated into equally large parts propagating in opposite directions, away from the oscillating body. This situation is related to the symmetry of the oscillating body in Figure 6.1.

Note that not only the amplitude but also the phase of the oscillation need to be optimum. If, say, the *b* and *c* curves had had opposite phases, then the right-hand half of the shown curve *d* would have had twice the amplitude of curve *a*. Then the immersed oscillating system would have functioned as an energy-delivering wave generator instead of an energy-receiving wave absorber.

It may perhaps seem like a paradox that a WEC need to produce an outgoing wave in order to receive incoming energy from the incident wave, but, as we have seen from the preceding illustration, this *is* a necessity if the WEC is to absorb any wave energy.

If, in contrast to the floating body indicated in Figure 6.1, the oscillating body is a submerged horizontal cylinder, its optimum oscillation requires the horizontal and vertical motions to have equal amplitudes, with phases differing by one quarter of a wave period. This is the principle utilised by the famous 'rotating Bristol cylinder' WEC. The cylinder axis performs a circular motion [71, 72].

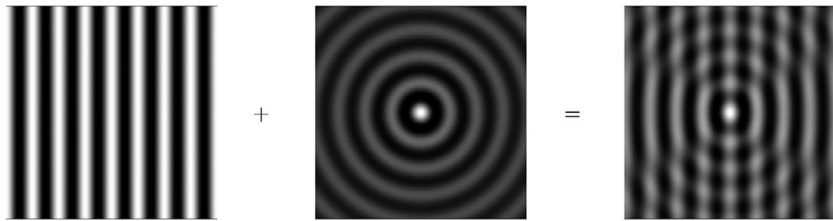


Figure 6.2: Snapshots of wave pattern of two interfering waves as seen from above. A plane wave, incident from the left-hand side, is interfering with an outgoing circular wave generated by an isotropically radiating system.

The sense of rotation of the cylinder axis determines whether the system acts as a device receiving energy from the incident wave or as a device supplying additional wave energy to the sea.

Contrary to the aforementioned symmetric WECs, if an immersed large body is sufficiently nonsymmetric, it may, theoretically, absorb up to 100% and performs with optimum oscillation in only one mode of motion. An example is the famous Salter Duck WEC, oscillating in the pitch mode [73].

The aforementioned examples correspond to the so-called two-dimensional WECs, which are discussed in more detail in Chapter 8.

The simplest three-dimensional WEC example that we may think of is an isotropically radiating WEC which is interacting with an incident plane wave, as illustrated by Figure 6.2. As with the two-dimensional examples discussed earlier, whether the wave interaction corresponds to energy removal or energy delivery depends on the relative differences of the amplitudes and phases of the two (plane and circular) waves. It has been shown [34, 70, 74, 75] that, with an incident plane wave, for which the wave-power level is  $J$ , as given by Eq. (4.130), the maximum converted power is

$$P_{\text{MAX}} = J/k = d_{a,\text{MAX}}J, \quad (6.1)$$

under conditions of optimum amplitude and phase relationships between the plane wave and the circular wave. Here,

$$d_{a,\text{MAX}} = 1/k = \lambda/2\pi \quad (6.2)$$

is the maximum *absorption width* for the isotropically radiating WEC. The quantity absorption width is defined as the ratio between  $P$  and  $J$  and is more commonly called *capture width*. A derivation of this result is given later in the present chapter; see Eqs. (6.13)–(6.15) and (6.103)–(6.104). Compare also Problem 4.16, where the interaction between a plane wave and a circular wave is discussed.

### 6.1.1 Classification of WEC Bodies

The isotropically radiating system in Figure 6.2 can for example be a heaving axisymmetric body. Such a WEC body was, in 1975, by Budal & Falnes [70]

called a *point absorber*, provided ‘its horizontal extension is much smaller than one wavelength’. To justify their assumption of negligible wave diffraction on the point absorber, we need to adopt Brian Count’s more precise definition of point absorbers as ‘structures that are small in comparison to the incident wavelength (say less than 1/20th of a wavelength)’ [76].

In contrast to point-absorber WECs, a *line-absorber* WEC has one of its two horizontal extensions at least as large as one wavelength, while the second horizontal extension is very much smaller than one wavelength. Traditionally, a line absorber is called a *terminator* if it is aligned perpendicular to the predominant propagation direction of the incident wave, and it is called an *attenuator* if it is parallel. Early examples of terminators are the Salter Duck and the Bristol Cylinder, while early examples of attenuators are the ship-like Kaime device and the flexible-bag device [76]. The two last-mentioned devices belong to the type of WECs discussed in Chapter 7.

So far, we have classified WECs having horizontal extension less than 1/20 of a wavelength and one wavelength or more as point absorbers and line absorbers, respectively. To bridge the gap between them, WECs which have a horizontal extension between 5% to 100% of a wavelength may be classified as *quasi-point absorbers (QPAs)* [77]. In contrast to point absorbers, wave diffraction is not negligible for QPAs.

If a semisubmerged body is oscillating in the heave mode, it displaces a water volume  $V_{\text{water}}$  when it moves downwards. When the body returns upwards, an equally large amount of water is sucked back. As a result of this local water motion, an outgoing wave is generated. This heaving body is a *monopole* or a ‘source’ type of wave radiator. If the body oscillates in the surge or pitch mode, it is a *dipole* type of wave radiator, corresponding to two monopoles of opposite signs, displaced horizontally from each other in the  $x$ -direction (see Figure 5.2). Also, sway and roll modes are dipole-type of wave radiators corresponding to two opposite monopoles displaced horizontally from each other in the  $y$ -direction. If the body oscillates in the yaw mode, it is a *quadrupole* type of wave radiator. This corresponds to two, horizontally displaced, dipole-type of wave radiators of opposite polarities. A fully submerged heaving body is a monopole type of wave radiator. Its net monopole strength, however, results from two partial monopole contributions of opposite signs, but displaced vertically from each other. The upper contribution to the net monopole strength is larger than the opposite lower contribution. The lower contribution is smaller.

Observe that point absorbers may preferably be monopole radiators, for example, heaving semisubmerged bodies or volume-varying submerged bodies. Depending on its horizontal extension, a QPA—in contrast to a point absorber—may possibly be a dipole radiator, operating in, for example, surge and/or pitch modes.

Our aim is to study the very important primary wave-energy conversion, the process of ocean-wave energy being converted to some unspecified mechanical

energy to be stored by a WEC. It is outside the scope of this book to discuss the secondary conversion of the absorbed energy to be used for chemical, mechanical or electrical applications, or the need to smooth out the large minute-to-minute variation of the incident wave energy, for which case an energy store is essential, for example, when delivering electric energy to a weak grid [5]. For recent reviews of practical wave-energy conversion efforts, see, for example, [9–11].

## 6.2 WEC Body Oscillating in One Mode

For simplicity, let us first consider a single body which has only one degree of motion, only heave ( $j = 3$ ) or only pitch ( $j = 5$ ), for example. An incident wave produces an excitation force  $\hat{F}_{e,j}$ . The body responds to this force by oscillating with a velocity  $\hat{u}_j$ . The total force is given by Eq. (5.155), which in this case simplifies to

$$\hat{F}_{t,j} = \hat{F}_{e,j} - Z_{jj}\hat{u}_j = f_j A - Z_{jj}\hat{u}_j, \quad (6.3)$$

where  $Z_{jj}$  is the body's radiation impedance,  $f_j$  is the excitation-force coefficient and  $A$  is the complex amplitude of the incident wave's elevation at the origin  $(x, y) = (0, 0)$ . If we multiply through this equation by  $\frac{1}{2}\hat{u}_j^*$  and take the real part, we obtain, according to Eq. (2.76), the time-averaged *absorbed power*

$$P = \frac{1}{2}\text{Re}\{\hat{F}_{t,j}\hat{u}_j^*\} = P_e - P_r, \quad (6.4)$$

where

$$P_e = \frac{1}{2}\text{Re}\{\hat{F}_{e,j}\hat{u}_j^*\} = \frac{1}{4}(f_j A \hat{u}_j^* + f_j^* A^* \hat{u}_j) \quad (6.5)$$

is the *excitation power* from the incident wave, and

$$P_r = \frac{1}{2}\text{Re}\{Z_{jj}\hat{u}_j\hat{u}_j^*\} = \frac{1}{2}R_{jj}|\hat{u}_j|^2 \quad (6.6)$$

is the *radiated power* due to the WEC body's oscillation. Here  $R_{jj} = \text{Re}\{Z_{jj}\}$  is the radiation resistance.

Note that the excitation power

$$P_e = \overline{\hat{F}_{e,j}(t)\hat{u}_j(t)} = \frac{1}{2}\text{Re}\{\hat{F}_{e,j}\hat{u}_j^*\} = \frac{1}{2}|\hat{F}_{e,j}||\hat{u}_j| \cos \gamma_j, \quad (6.7)$$

where  $\gamma_j = \varphi_u - \varphi_F$  is the phase difference between  $\hat{u}_j$  and  $\hat{F}_{e,j}$ , is linear in  $u_j$ , whereas the radiated power

$$P_r = -\overline{\hat{F}_{r,j}(t)\hat{u}_j(t)} = \frac{1}{2}R_{jj}|\hat{u}_j|^2 \quad (6.8)$$

is quadratic in  $u_j$ , since  $F_{r,j}$  is linear in  $u_j$ . Thus, a graph of  $P$  versus  $|\hat{u}_j|$  is a parabola, as indicated in Figure 6.3. We observe that in order to absorb wave power (that is,  $P > 0$ , or,  $P_e > P_r$ ), it is necessary that  $|\gamma_j| < \pi/2$  and also that  $0 < |\hat{u}_j| < (|\hat{F}_{e,j}|/R_{jj}) \cos \gamma_j$ . The optimum phase angle is  $\gamma_{j,\text{opt}} = 0$ .

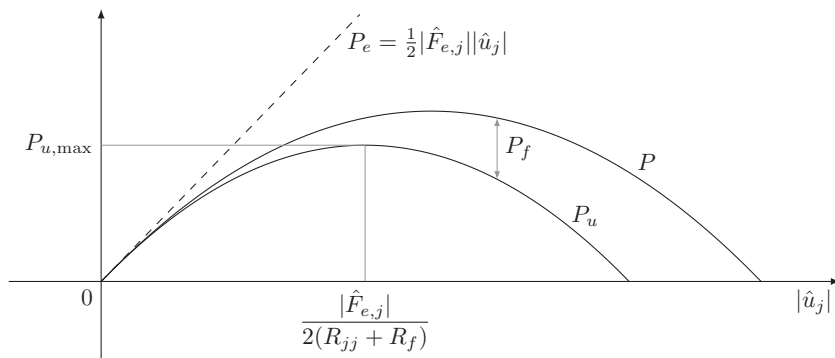


Figure 6.3: Curves showing absorbed wave power  $P$ , useful power  $P_u$  and excitation power  $P_e$  versus velocity amplitude  $|u_j|$  at optimum phase angle  $\gamma_{j,\text{opt}} = 0$ .

Hence, a certain fraction of the excitation power  $P_e$  arriving at the oscillating body is necessarily returned to the sea as radiated power  $P_r$ . Wave interference is a clue to the explanation of this fact. The radiated wave interferes destructively with the incident wave. The resulting wave, which propagates beyond the wave absorber, transports less power than the incident wave. The radiated power  $P_r$  should be considered as a necessity rather than as a loss.

### 6.2.1 Maximum Absorbed Wave Power

For a given body and a given incident wave, the excitation force  $F_{e,j}$  is a given quantity. Let us discuss how the absorbed power  $P$  depends on the oscillating velocity  $u_j$ .

Observing Eqs. (6.7)–(6.8), we note the following. The optimum velocity amplitude is

$$|\hat{u}_{j,\text{opt}}| = \frac{|\hat{F}_{e,j}|}{2R_{jj}} \cos \gamma_j, \quad (6.9)$$

giving the maximum absorbed power

$$P_{\max} = \frac{|\hat{F}_{e,j}|^2}{8R_{jj}} \cos^2 \gamma_j = P_{r,\text{opt}} = \frac{1}{2} P_{e,\text{opt}}. \quad (6.10)$$

With this optimum condition, the radiated power is as large as the absorbed power. Note that, for the case of resonance ( $\gamma_j = 0$ ), we write (as in the following paragraphs)  $P_{\max}$  and  $\hat{u}_{j,\text{opt}}$  instead of  $P_{\max}$  and  $\hat{u}_{j,\text{opt}}$ .

It can be shown (see Problem 6.5) that  $P_{\max}$  as given by Eq. (6.10) is greater than  $P_{a,\max}$ , as given by Eq. (3.41), except that they are equally large when  $\gamma_j = 0$ —that is, at resonance. The reason why  $P_{a,\max}$  may be smaller than  $P_{\max}$  is that in the former case, the oscillation amplitude is restricted by the simple dynamic equation (3.30), whereas  $\hat{u}_j$  in the present section is considered

as a quantity to be freely selected. Thus, in order to realise the optimum  $\hat{u}_j$ , it may be necessary to include a control device in the oscillation system. On this assumption, we may consider  $\hat{u}_j$  to be an independent variable. The *optimum* value  $\hat{u}_{j,\text{OPT}}$ , however, depends on the excitation force  $\hat{F}_{ej} = f_j(\beta)A$ , and, consequently, on the incident-wave parameters  $A$  and  $\beta$ .

Assuming that, in addition to selecting the optimum amplitude according to Eq. (6.9), we also select the optimum phase  $\gamma_j = 0$ —that is, an optimum complex amplitude

$$\hat{u}_{j,\text{OPT}} = \frac{\hat{F}_{ej}(\beta)}{2R_{jj}} = \frac{f_j(\beta)A}{2R_{jj}}, \quad (6.11)$$

then the maximum absorbed power is

$$P_{\text{MAX}} = \frac{|\hat{F}_{ej}(\beta)|^2}{8R_{jj}} = P_{r,\text{OPT}} = \frac{1}{2}P_{e,\text{OPT}}. \quad (6.12)$$

Note that here  $P_{\text{MAX}}$  agrees with Eq. (3.45), which is applicable at resonance.

If the oscillation amplitude is twice that of the optimum value given by Eq. (6.11), then the absorbed wave power is zero,  $P = 0$ , and  $P_r = P_e = 4P_{\text{MAX}}$ . This is the situation when a linear array of resonant (that is,  $\gamma_j = 0$ ) heaving slender bodies—or one single body in a narrow wave channel (see Figure 6.1)—is used as a dynamic wave reflector [78]. Then the radiated wave cancels the transmitted wave on the downwave side of the oscillating body. On the upwave side, a standing wave occurs, resulting from superposition of the radiated and incident waves with approximately equal amplitudes but opposite propagation directions.

We may now use Eq. (5.145) to express the radiation resistance in terms of the excitation force. Then we have

$$P_{\text{MAX}} = \frac{|\hat{F}_{ej}(\beta)|^2}{8R_{jj}} = \frac{2\pi J |\hat{F}_{ej}(\beta)|^2}{k \int_{-\pi}^{\pi} |\hat{F}_{ej}(\beta')|^2 d\beta'} = \frac{J}{k} G_j(\beta) = \frac{\lambda}{2\pi} J G_j(\beta), \quad (6.13)$$

where

$$G_j(\beta) = \frac{2\pi |\hat{F}_{ej}(\beta)|^2}{\int_{-\pi}^{\pi} |\hat{F}_{ej}(\beta')|^2 d\beta'} = \frac{2\pi |f_j(\beta)|^2}{\int_{-\pi}^{\pi} |f_j(\beta')|^2 d\beta'} = \frac{2\pi |h_j(\beta \pm \pi)|^2}{\int_{-\pi}^{\pi} |h_j(\beta' \pm \pi)|^2 d\beta'}. \quad (6.14)$$

Here, in the last step, we have made use of Eq. (5.142). Observe that this *optimum power-gain function*  $G_j(\beta)$  is applicable only when  $P = P_{\text{MAX}}$ , and not, in general, when  $P < P_{\text{MAX}}$ .

For an immersed body with a vertical axis of symmetry, it follows, from Eqs. (5.285)–(5.287) and (6.14), that the optimum power-gain functions are  $G_1(\beta) = G_5(\beta) = 2\cos^2\beta$  for the surge and pitch modes,  $G_2(\beta) = G_4(\beta) = 2\sin^2\beta$  for the sway and roll modes, and  $G_3(\beta) \equiv 1$  for the heave mode. Except for the heave mode, which is the simplest case, these optimum power-gain functions were first derived by Newman [34].

Averaging the optimum power-gain function  $G_j(\beta)$  as defined by Eq. (6.14) over all horizontal wave-incidence angles  $\beta$ , we obtain

$$G_{j,\text{average}} = 1, \quad (6.15)$$

except for singular cases where  $G_{j,\text{average}} = 0$ . We have such an exceptional case, for instance, with the yaw mode ( $j = 6$ ) for an immersed body that has a vertical axis of symmetry. Moreover, if such a body has a shape with a relatively small water-plane area, as indicated on Figure 5.16, we may, for one particular frequency, have  $G_{3,\text{average}} = 0$  because  $h_3 = 0$  for this frequency.

For the case of deep water, the wavelength  $\lambda$  and the wave-power level  $J$  are given by Eqs. (4.100) and (4.131), respectively. Thus, for this case, we find from Eq. (6.13) the simple formula

$$P_{\text{MAX}} = c_j H^2 T^3, \quad (6.16)$$

where

$$c_j = c_j(\beta) = G_j(\beta) \rho g^3 / 128\pi^3 = (245 \text{ W m}^{-2}\text{s}^{-3}) G_j(\beta), \quad (6.17)$$

for the immersed WEC body oscillating in mode  $j$ .

### 6.2.2 Converted Useful Power

The wave power  $P$  which is converted by a WEC body is divided between converted useful power  $P_u$  and an unavoidable lost power  $P_f$  due to viscous effects, friction and non-ideal energy-conversion equipment.

For simplicity, we consider a power takeoff system with linear characteristics, as indicated schematically in Figure 6.4, where resistance  $R_f$  is associated with the lost power [see Eq. (5.340)]. In a similar way, we introduce a load resistance  $R_u$ , corresponding to the useful power, such that the load force  $F_{u,j}$  [see Eqs. (5.339) and (5.344)] is

$$F_{u,j} = -R_u u_j. \quad (6.18)$$

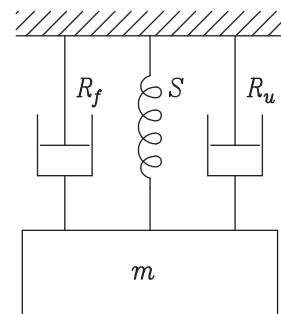


Figure 6.4: Schematic model of a linear power takeoff system of an oscillating system. Mechanical resistances  $R_u$  and  $R_f$  account for converted useful power and power lost by friction and viscous damping, respectively.

Mass  $m$  includes the mass of the oscillating body, and stiffness  $S$  includes the hydrostatic buoyancy effect. Radiation resistance  $R_{jj}$  and added mass  $m_{jj}$  are not shown in the schematic diagram of Figure 6.4.

The lost power is

$$P_f = \frac{1}{2}R_f|\hat{u}_j|^2, \quad (6.19)$$

and the *useful power* is

$$\begin{aligned} P_u &= \frac{1}{2}R_u|\hat{u}_j|^2 = P - P_f = P_e - (P_r + P_f) \\ &= \frac{1}{2}|\hat{F}_{e,j}||\hat{u}_j| \cos \gamma_j - \frac{1}{2}(R_{jj} + R_f)|\hat{u}_j|^2. \end{aligned} \quad (6.20)$$

For the particular case of  $\gamma_j = 0$ , corresponding to optimum phase, a graphical representation of  $P_u$ ,  $P$ ,  $P_e$  and  $P_f$  versus  $|\hat{u}_j|$  are given in the diagram of Figure 6.3. If

$$\hat{u}_j = \hat{F}_{e,j}/(2(R_{jj} + R_f)), \quad (6.21)$$

that is, if  $\gamma_j = 0$  and  $|\hat{u}_j| = |\hat{F}_{e,j}|/(2(R_{jj} + R_f))$ , then we have the maximum useful power

$$P_{u,\text{MAX}} = |\hat{F}_{e,j}|^2/(8(R_{jj} + R_f)). \quad (6.22)$$

Note that a lower oscillation amplitude is required to obtain maximum useful power than to obtain the maximum absorbed wave power. The phase condition  $\gamma_j = 0$  for optimum is the same in both cases. The velocity has to be in phase with the excitation force.

In the preceding discussion, we have assumed that  $\hat{u}_j$  is a variable at our disposal; that is, we may choose  $|\hat{u}_j|$  and  $\gamma_j$  as we like. To achieve the desired value(s), it may be necessary to provide the dynamic system with a certain device for power takeoff and oscillation control. This device supplies a ‘load’ force  $F_{u,j}$  in addition to the excitation force  $F_{e,j}$ . In analogy with Eq. (5.350), the oscillation velocity has to obey the equation

$$Z_i(\omega)\hat{u}_j = \hat{F}_{e,j} + \hat{F}_{u,j}, \quad (6.23)$$

where  $Z_i(\omega)$  is the intrinsic mechanical impedance for oscillation mode  $j$ . It is the mechanical impedance of the oscillating system, and it includes the radiation impedance but not the effects of the mentioned device for control and power takeoff. These effects are represented by the last term  $\hat{F}_{u,j}$  in Eq. (6.23). As an extension of Eq. (6.18), let us now assume that the load force may be written as

$$\hat{F}_{u,j} = -Z_u(\omega)\hat{u}_j, \quad (6.24)$$

where  $Z_u(\omega)$  is a load impedance. Introducing this into Eq. (6.23) gives

$$[Z_i(\omega) + Z_u(\omega)]\hat{u}_j = \hat{F}_{e,j}. \quad (6.25)$$

The converted useful power is

$$\begin{aligned} P_u &= \frac{1}{2} \operatorname{Re}\{-\hat{F}_u \hat{u}_j^*\} = \frac{1}{2} \operatorname{Re}\{Z_u(\omega)\} |\hat{u}_j|^2 \\ &= \frac{1}{2} \operatorname{Re}\{Z_u(\omega)\} \frac{|\hat{F}_{ej}|^2}{|Z_i(\omega) + Z_u(\omega)|^2} \\ &= \frac{R_u(\omega) |\hat{F}_{ej}|^2 / 2}{(R_i(\omega) + R_u(\omega))^2 + (X_i(\omega) + X_u(\omega))^2}, \end{aligned} \quad (6.26)$$

where we, in the last step, have split the impedances  $Z(\omega)$  into real parts  $R(\omega)$  and imaginary parts  $X(\omega)$ . Note that the last expression here agrees with Eq. (3.39). Utilising the results of Eqs. (3.42) and (3.44), we find that the optimum values for  $R_u(\omega)$  and  $X_u(\omega)$  are  $R_i(\omega)$  and  $-X_i(\omega)$ , respectively. Hence, for

$$Z_u(\omega) = Z_i^*(\omega) \equiv Z_{u,\text{OPT}}(\omega), \quad (6.27)$$

we have the maximum useful power [in agreement with Eq. (6.22)]

$$P_u = \frac{|\hat{F}_{ej}|^2}{8R_i} \equiv P_{u,\text{MAX}}. \quad (6.28)$$

Note that the reactive part of the total impedance is cancelled under the optimum condition. This is automatically fulfilled in the case of resonance. Moreover, under the optimum condition, we have resistance matching, that is,  $R_u(\omega) = R_i(\omega)$ .

### 6.2.3 The Wave-Power ‘Island’

We consider an incident plane wave propagating on deep water or on water of constant depth. Let its complex wave-elevation amplitude be

$$\hat{\eta} = A e^{-ik(x \cos \beta + y \sin \beta)} = A e^{-ikr \cos(\beta - \theta)}, \quad (6.29)$$

as expressed in Cartesian coordinates  $(x, y, z)$  and, alternatively, in cylindrical coordinates  $(r, \theta, z)$ ; thus,  $x = r \cos \theta$  and  $y = r \sin \theta$ . The plane wave’s propagation direction is at an angle  $\beta$  with respect to the  $x$ -axis, and its complex elevation amplitude at the origin is  $A$ .

Let us now assume that an immersed WEC body is oscillating in one mode, mode  $j$ , for instance. We define two quantities  $U$  and  $E(\beta)$ , as follows:

$$|U|^2 = UU^* = R_{jj} \hat{u}_j \hat{u}_j^*/2 = P_r = \frac{\omega \rho v_p v_g}{4\pi g} \int_0^{2\pi} h_j(\theta) h_j^*(\theta) d\theta \hat{u}_j \hat{u}_j^* \quad (6.30)$$

$$E(\beta) = f_{ej}(\beta) \hat{u}_j^*/4 = (\rho v_p v_g / 2) h_j(\beta + \pi) \hat{u}_j^*, \quad (6.31)$$

where we in the last step have made use of Eqs. (5.135), (5.142) and (4.107).

In Eq. (6.30), the nonnegative quantity  $P_r$  represents the radiated wave power (caused by any forced oscillation of the immersed body). Note that

the introduced complex quantity  $U = \sqrt{P_r}e^{i\delta}$  may have any arbitrary phase angle  $\delta$  in the interval  $-\pi < \delta \leq \pi$  of the complex plane. We shall find it convenient, however, to choose  $U$  to have the same phase angle as  $A^*E^*(\beta)$ . Then  $A^*E^*(\beta)/U$  is a real positive quantity, which, notably, is independent of the complex velocity amplitude  $\hat{u}_j$ .

We may now simplify Eqs. (6.4)–(6.6) for the time-average absorbed wave power to

$$P = P_e - P_r = AE(\beta) + A^*E^*(\beta) - |U|^2. \quad (6.32)$$

By simple algebraic manipulation of Eq. (6.32), we may show that

$$P = |AE(\beta)/U^*|^2 - |U - AE(\beta)/U^*|^2, \quad (6.33)$$

from which simply by inspection we see that the first term equals the maximum possible absorbed power, provided the last term vanishes—that is, if the quantities  $U$  and  $E(\beta)$  have optimum values  $U_0$  and  $E_0(\beta)$  satisfying the optimum condition

$$U_0 - AE_0(\beta)/U_0^* = 0, \quad \text{that is, } AE_0(\beta) = |U_0|^2 = A^*E_0^*(\beta). \quad (6.34)$$

Thus, evidently, we have several different alternative expressions for the maximum absorbed power—for example,

$$P_{\text{MAX}} = P_{r,\text{OPT}} = |U_0|^2 = P_{e,\text{OPT}}/2 = AE_0(\beta) = A^*E_0^*(\beta) = |AE_0(\beta)|; \quad (6.35)$$

see also Eq. (6.12).

As we have chosen  $A^*E^*(\beta)/U$  to be a real positive quantity which is independent of  $u_i$  and, therefore, also of  $U$ , we have

$$\frac{A^*E^*(\beta)}{U} = \frac{A^*E_0^*(\beta)}{U_0} = U_0^* = U_0^*(\beta) = |U_0(\beta)| = U_0(\beta), \quad (6.36)$$

where we have made use of the optimum condition (6.34). In general, we shall consider  $U$  to be an independent complex oscillation-state variable, while the optimum value  $U_0(\beta)$  is real and positive, because we have chosen  $U$  to have the same phase as  $A^*E^*(\beta)$ . According to Eq. (6.36), we have  $A^*E^*(\beta) = U_0^*U$  and  $AE(\beta) = U_0U^*$ . If we insert this into Eq. (6.32) and also use Eq. (6.35), we obtain the simple equation

$$P_{\text{MAX}} - P = U_0U_0^* - U_0U^* - U_0^*U + UU^* = |U_0 - U|^2 = |U_0(\beta) - U|^2, \quad (6.37)$$

which, for a fixed value  $P < P_{\text{MAX}}$ , corresponds to the equation of a circle of radius  $\sqrt{P_{\text{MAX}} - P}$  centred at  $U_0(\beta)$  in the complex  $U$  plane. Equation (6.37) may be illustrated as an axisymmetric paraboloid, the wave-power ‘island’, in a diagram where a vertical real  $P$  axis is erected on a horizontal complex  $U$  plane, as shown in Figure 6.5. The upper parabola shown in Figure 6.3 corresponds

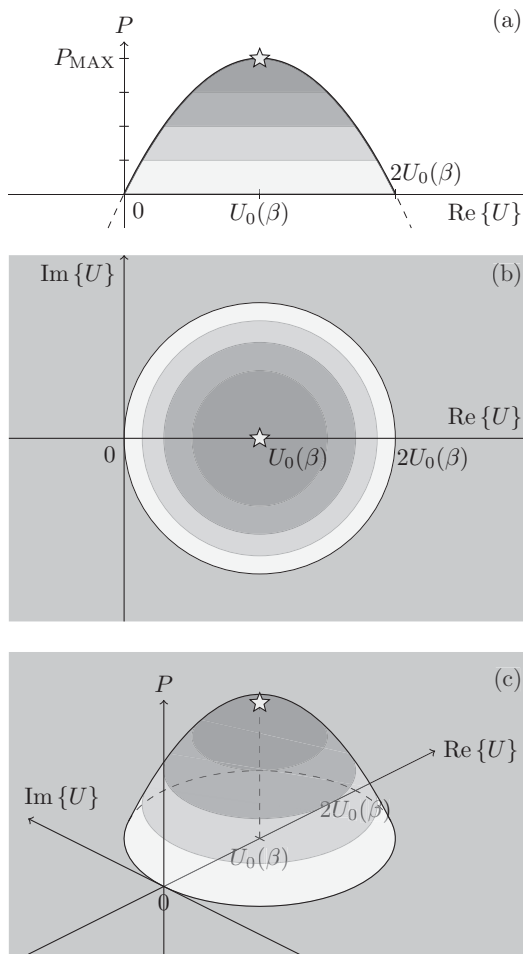


Figure 6.5: The wave-power ‘island’. Absorbed wave power  $P$  as a function of the complex collective oscillation amplitude  $U = \text{Re}\{U\} + i\text{Im}\{U\} = |U|e^{i\delta}$ , where the phase  $\delta = \arg\{U\}$  is chosen to satisfy Eq. (6.36), and where  $|U|$  is given by Eq. (6.30) for the one-mode oscillating-body case, and by Eq. (8.74) for the case of a general WEC array. The largest possible absorbed wave power  $P_{\text{MAX}}$  is indicated by a star on the top of the axisymmetric paraboloid, and  $U_0$  is the optimum collective oscillation amplitude. Colour changes indicate levels where  $P/P_{\text{MAX}}$  equals 1/4, 1/2 and 3/4. (a) Side view. (b) Top view. (c) Inclined view. For a colour version of the figure, see figure 1 of [63], accessible at <https://doi.org/10.1098/rsos.140305>.

to an intersection between the paraboloid and a vertical plane through the real vertical  $P$  axis and the real axis of the horizontal complex  $U$  plane. If this vertical plane makes an angle  $\gamma_j$  with the real  $U$  axis, then the intersection is a lower parabola with a maximum corresponding to Eq. (6.10).

As will be shown later in this book, by generalising the definition of the complex quantities  $U$  and  $E(\beta)$ , the simple formula (6.37), as well as the wave-power ‘island’, is applicable to oscillating water columns (OWCs) and even to arrays of WEC bodies and OWCs.

### 6.3 Optimum Control of a WEC Body

The purpose of this section is to study wave-energy conversion when the waves are not sinusoidal and to discuss conditions for maximising the converted energy. For simplicity, we are discussing oscillation in only one mode—for instance, heave ( $j = 3$ ) or pitch ( $j = 5$ ). Thus, we shall omit the subscript  $j$  in the present section. Replacing the complex amplitudes  $\hat{u}$ ,  $\hat{F}_e$ , and  $\hat{F}_u$  by the corresponding Fourier transforms  $u(\omega)$ ,  $F_e(\omega)$  and  $F_u(\omega)$ , we may write Eq. (6.23) as

$$Z_i(\omega)u(\omega) = F_e(\omega) + F_u(\omega) = F_{\text{ext}}(\omega). \quad (6.38)$$

We rewrite the corresponding time-domain equation as

$$z_i(t) * u_t(t) = F_{e,t}(t) + F_{u,t}(t), \quad (6.39)$$

which for the heave mode specialises to Eq. (5.361). The causal impulse-response function  $z_i(t)$  is the inverse Fourier transform of the intrinsic mechanical impedance  $Z_i(\omega)$ ; see Section 5.9.

In analogy with Eq. (6.8), the average useful power is  $P_u = -\overline{F_{u,t}(t)u_t(t)}$ , and thus, the converted useful energy is

$$W_u = - \int_{-\infty}^{\infty} F_{u,t}(t)u_t(t) dt. \quad (6.40)$$

(This integral exists if the integrand tends sufficiently fast to zero as  $t \rightarrow \pm\infty$ .) By applying the frequency convolution theorem (2.148) for  $\omega = 0$  and utilising the fact that  $F_{u,t}(t)$  and  $u_t(t)$  are real, we obtain, in analogy with Eqs. (2.201) and (2.205), that

$$W_u = \frac{1}{2\pi} \int_0^{\infty} \{-F_u(\omega)u^*(\omega) - F_u^*(\omega)u(\omega)\} d\omega. \quad (6.41)$$

By algebraic manipulation of the integrand, we may rewrite this as

$$\begin{aligned} W_u &= \frac{1}{2\pi} \int_0^{\infty} \left\{ \frac{|F_e(\omega)|^2}{2R_i(\omega)} - \left[ \frac{F_e(\omega)F_e^*(\omega)}{2R_i(\omega)} + F_u(\omega)u^*(\omega) + F_u^*(\omega)u(\omega) \right] \right\} d\omega \\ &= \frac{2}{\pi} \int_0^{\infty} \left\{ \frac{|F_e(\omega)|^2}{8R_i(\omega)} - \frac{\alpha(\omega)}{8R_i(\omega)} \right\} d\omega, \end{aligned} \quad (6.42)$$

where

$$\alpha(\omega) = F_e(\omega)F_e^*(\omega) + 2R_i(\omega)[F_u(\omega)u^*(\omega) + F_u^*(\omega)u(\omega)]. \quad (6.43)$$

Here  $F_e(\omega)$  is the Fourier transform of the excitation force  $F_{e,t}(t)$ , and

$$R_i(\omega) = \frac{Z_i(\omega) + Z_i^*(\omega)}{2} \quad (6.44)$$

is the intrinsic mechanical resistance—that is, the real part of the intrinsic mechanical impedance. In the following, we shall prove that  $\alpha(\omega) \geq 0$ , and we

shall examine under which optimum conditions we have  $\alpha(\omega) \equiv 0$ . Then, since  $R_i(\omega) > 0$ , Eq. (6.42) means that the maximum converted useful energy is

$$W_{u,\text{MAX}} = \frac{2}{\pi} \int_0^\infty \frac{|F_e(\omega)|^2}{8R_i(\omega)} d\omega \quad (6.45)$$

under the condition that  $\alpha(\omega) = 0$  for all  $\omega$ . Otherwise, we have, in general,

$$W_u = W_{u,\text{MAX}} - W_{u,P}, \quad (6.46)$$

where

$$W_{u,P} = \frac{2}{\pi} \int_0^\infty \frac{\alpha(\omega)}{8R_i(\omega)} d\omega, \quad (6.47)$$

which is a lost-energy penalty for not operating at optimum. Observe that  $W_{u,P} \geq 0$ . We wish to minimise  $W_{u,P}$  and, if possible, reduce it to zero. It can be shown that Eq. (6.28), which applies for the case of a sinusoidal wave, is in agreement with Eq. (6.45); see Problem 2.14.

In order to show that  $\alpha \geq 0$ , we shall make use of the dynamic equation (6.38) to eliminate either  $F_e(\omega)$  or  $F_u(\omega)$  from Eq. (6.43).

Omitting for a while the argument  $\omega$ , we find that Eq. (6.38) gives  $F_e = Z_i u - F_u$ , and thus,

$$F_e F_e^* = F_u F_u^* + Z_i Z_i^* u u^* - F_u Z_i^* u^* - F_u^* Z_i u. \quad (6.48)$$

Further, using Eq. (6.44), we have

$$\begin{aligned} 2R_i(F_u u^* + F_u^* u) &= (Z_i + Z_i^*)(F_u u^* + F_u^* u) \\ &= F_u Z_i u^* + F_u^* Z_i^* u + F_u Z_i^* u^* + F_u^* Z_i u. \end{aligned} \quad (6.49)$$

Inserting these two equations into Eq. (6.43) gives

$$\alpha = F_u F_u^* + Z_i Z_i^* u u^* + F_u Z_i u^* + F_u^* Z_i^* u = (F_u + Z_i^* u)(F_u^* + Z_i u^*). \quad (6.50)$$

Hence, we have

$$\alpha(\omega) = |F_u(\omega) + Z_i^*(\omega)u(\omega)|^2 \geq 0, \quad (6.51)$$

and from this, we see that the optimum condition is

$$F_u(\omega) = -Z_i^*(\omega)u(\omega), \quad (6.52)$$

which for sinusoidal waves and oscillations agrees with Eqs. (6.24) and (6.27).

Eliminating differently, we have  $F_u = Z_i u - F_e$  from the dynamic equation (6.38), which by insertion into Eq. (6.43) gives

$$\begin{aligned} \alpha &= F_e F_e^* + 2R_i(Z_i u u^* - F_e u^* + Z_i^* u u^* - F_e^* u) \\ &= F_e F_e^* + (2R_i)^2 u u^* - F_e 2R_i u^* - F_e^* 2R_i u \\ &= (F_e - 2R_i u)(F_e^* - 2R_i u^*) \end{aligned} \quad (6.53)$$

when Eq. (6.44) has also been observed. Hence, we have

$$\alpha(\omega) = |F_e(\omega) - 2R_i(\omega)u(\omega)|^2 \geq 0. \quad (6.54)$$

From this second proof of the relation  $\alpha \geq 0$ , we obtain the optimum condition written in the alternative way:

$$u(\omega) = \frac{F_e(\omega)}{2R_i(\omega)}, \quad (6.55)$$

which for sinusoidal waves and oscillations agrees with Eq. (6.11).

### 6.3.1 Methods for Optimum Control

The two alternative ways to express the optimum condition, as Eq. (6.52) or as Eq. (6.55), have been used for quite some time. To achieve the optimum condition (6.52) has been called *reactive control* [79] or *complex-conjugate control* [80], and it was already in the mid-1970s tested experimentally in sinusoidal waves [81]. ‘Reactive control’ refers to the fact that the optimum reactance  $X_u$  (the imaginary part of  $Z_u = -F_u/u$ ) cancels the reactance  $X_i$  (the imaginary part of  $Z_i$ ). ‘Complex-conjugate control’ refers to the fact that the optimum load impedance  $Z_u$  equals the complex conjugate of the intrinsic impedance  $Z_i$ . On the other hand, to achieve the optimum condition (6.55) has been called *phase control* and *amplitude control* [74] because condition (6.55) means, firstly, that the oscillation velocity  $u$  must be in phase with the excitation force  $F_e$  and, secondly, that the velocity amplitude  $|u|$  must equal  $|F_e|/2R_i$ . A similar method was proposed and investigated before 1970 [82]. Then an attempt was made to achieve optimum oscillation on the basis of wave measurement at an ‘upwave’ position in a wave channel. In this particular case, the object was not to utilise the wave energy but to achieve complete wave absorption in a wave channel.

We should note that in order to obtain the optimum condition  $\alpha(\omega) \equiv 0$ , unless  $Z_i$  is real, it is necessary that reactive power is involved to achieve optimum. This means that the load-and-control machinery which supplies the load force  $F_u$  not only receives energy but also must return some energy during part of the oscillation cycle. (The final part of Section 2.3.1 helps us understand this fact.) Obviously, it is desirable that this machinery has a very high energy-conversion efficiency (preferably close to 1). If, for some reason, we do not want or are unable to return the necessary amount of energy, then we have a suboptimal control, for which  $\alpha(\omega) \neq 0$  and, hence,  $W_{u,P} > 0$  [see Eq. (6.47)].

An example of such a suboptimal method is phase control by latching, a principle [78, 83] that is illustrated by Figure 6.6 for a heaving body which is so small that the excitation force is in phase with the incident wave elevation (sinusoidal in this case). By comparing curves *b* and *c* in Figure 6.6, it is obvious that if the resonance (curve *b*) represents optimum in agreement with condition (6.55), then the latching phase control (curve *c*) is necessarily suboptimal.

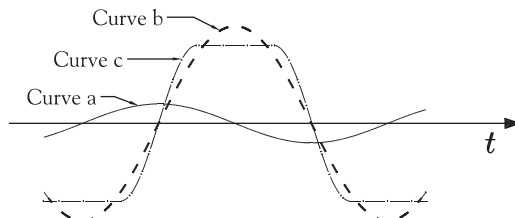


Figure 6.6: Resonance and phase control. The curves indicate incident wave elevation and vertical displacement of (different versions of) a heaving body as functions of time. Curve a: Elevation of the water surface due to the incident wave (at the position of the body). This would also represent the vertical position of a body with negligible mass. For a body of diameter very small compared with the wavelength, curve a also represents the wave's heave force on the body. Curve b: Vertical displacement of heaving body whose mass is so large that its natural period is equal to the wave period (resonance). Curve c: Vertical displacement of a body with smaller mass and, hence, shorter natural period. Phase control is then obtained by keeping the body in a fixed vertical position during certain time intervals.

With latching-phase-control experiments in [84, 85], means have not been provided to enable the power takeoff machinery to return any energy during parts of the oscillation cycle.

An overview of the problem of optimum control for maximising the useful energy output from a physical dynamic system represented by Eq. (6.38) is illustrated by the block diagram in Figure 6.7. The oscillation velocity  $u$  is the system's response to the external force input  $F_{\text{ext}} = F_e + F_u$ . A switch in the block diagram indicates the possibility to select between two alternatives to determine the optimum load force  $F_u$ . One alternative is the reactive-control (or complex-conjugate-control) method corresponding to optimum condition (6.52). The other alternative is the amplitude-phase-control method corresponding to optimum condition (6.55), for which knowledge on the wave excitation force  $F_e$  is used to determine the optimum oscillation velocity  $u_{\text{opt}} = F_e/2R_i$ , which is compared with the measured actual velocity  $u$ . The deviation between  $u$  and  $u_{\text{opt}}$  is used as input to an indicated (but here not specified) controller, which provides the optimum load force  $F_u$ . This alternative control method, contrary to the reactive-control method, requires knowledge on the excitation force  $F_e$ .

The other switch in the block diagram of Figure 6.7 indicates the possibility to select between two alternatives to determine the excitation force from measurement either of the total wave force  $F_w = F_e + F_r = F_e - Z_r u$  acting on the dynamic system (Figure 6.8) or of the incident wave elevation  $A$  at a reference position some distance away from the system (Figure 6.9). Even if this position is upstream (referred to the wave propagation direction), the excitation force coefficient  $f_e(\omega)$  may correspond to a noncausal impulse-response function [37]. (See also Section 5.3.2.)

The two switches for choice of alternatives indicated in the block diagram of Figure 6.7 represent a redundancy if equipment is installed so that two methods are available both to determine  $F_e$  and to determine  $F_u$ . Obtained alternative

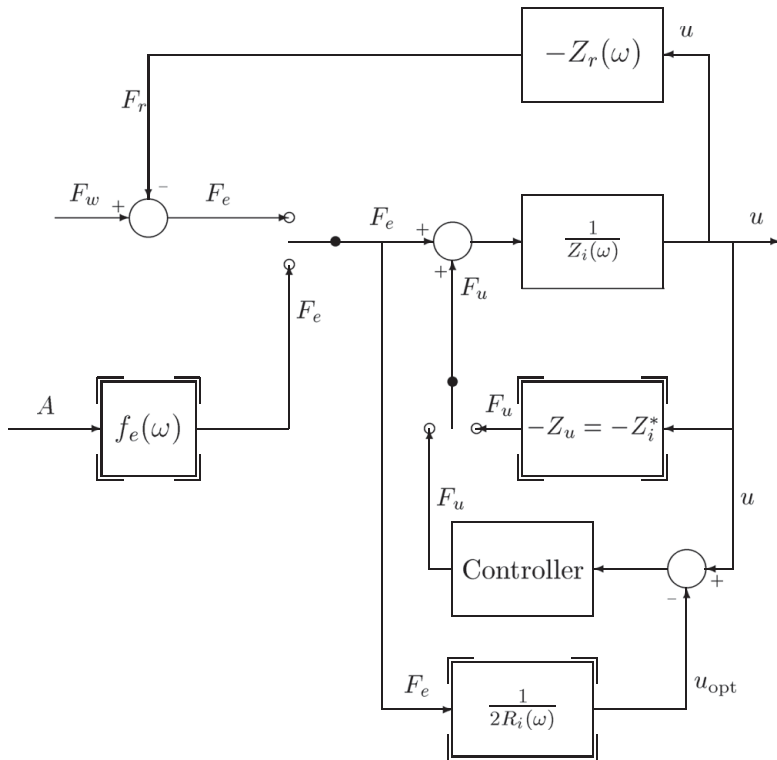


Figure 6.7: Block diagram overview of the control problem for maximising the converted energy by a system represented by the transfer function  $1/Z_i(\omega)$ , where the external force  $F_{ext} = F_e + F_u$  is the input and the velocity  $u$  the response. Two possibilities are indicated to determine both the excitation force  $F_e = f_eA = F_w - F_r$  and the optimum load force. Three of the blocks, which are marked by a hook on each corner, represent noncausal systems.

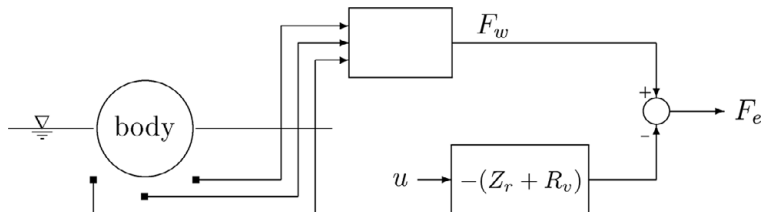


Figure 6.8: Pressure transducers placed on or near the wet surface of the immersed body may be used for measurement of the hydrodynamic pressure in order to estimate the total wave force  $F_w$  on the body. Deducting from  $F_w$  a wave force  $-(Z_r + R_v)u$  due to the body oscillation, the wave excitation force  $F_e$  is obtained.

results may then be compared. Such a redundancy may be useful if it is difficult to achieve a satisfactory optimum control in practice.

Figure 6.9 illustrates the situation if a measurement of wave elevation is chosen to be the method used for determining the excitation force  $F_e$  and if the amplitude-and-phase-control method is chosen in order to maximise the useful power.

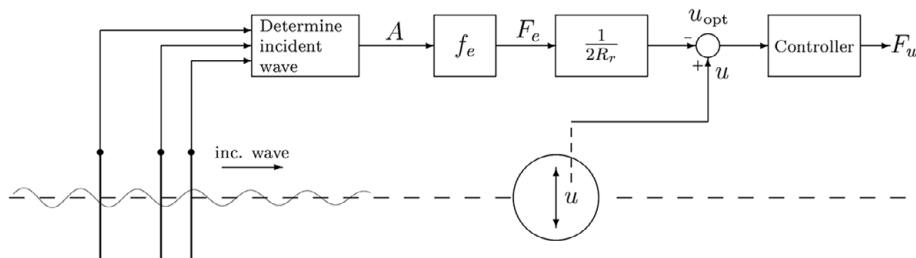


Figure 6.9: Measurement of incident wave elevation  $A$ , at some distance from the immersed body, for determination of the excitation force  $F_e = f_e A$  and of the optimum oscillation velocity  $u_{\text{opt}} = F_e / 2R_i$ , whose deviation from the measured actual velocity  $u$  is utilised as a signal to a controller for supplying the correct load force  $F_u$  to the immersed body.

A method for a more direct measurement of the total wave force  $F_w$  is indicated in Figure 6.8. An array of pressure transducers is placed on the wet body surface or in fixed positions near this surface. From measurement of the pressure in the fluid, the force  $F_w$  may be estimated using Eq. (5.21). If the body velocity  $u$  is also measured, the wave excitation force  $F_e$  may be estimated from

$$F_e = F_w - F_r - F_v + [-F_b] = F_w + Z_r u + R_v u + [S_b s], \quad (6.56)$$

where  $Z_r$  is the radiation impedance (as in the uppermost block of Figure 6.7) and  $R_v$  is the viscous resistance (as in Section 5.9). Moreover,  $s(\omega) = u(\omega)/i\omega$  is the Fourier transform of the displacement. Observe that, compared with the uppermost block in Figure 6.7, we have in Figure 6.8 made the generalisation of replacing  $Z_r$  with  $Z_r + R_v$ . The terms within the brackets in Eq. (6.56) should be included if the pressure transducers indicated in Figure 6.8 are placed on the body's wet surface and excluded if they are placed in fixed position in the water.

Let us next discuss the significance of the optimum conditions (6.52) and (6.55) in the time domain. Obviously  $z_i(t)$ , the inverse Fourier transform of  $Z_i(\omega)$ , is a causal function (cf. Subsection 5.9.1). Thus, in agreement with Eqs. (2.176)–(2.179), we have the following. Let

$$\mathcal{F}^{-1}\{Z_i(\omega)\} = z_i(t) = r_i(t) + x_i(t) = \begin{cases} 2r_i(t) & \text{for } t > 0 \\ r_i(0) & \text{for } t = 0, \\ 0 & \text{for } t < 0 \end{cases} \quad (6.57)$$

where the even and odd parts of  $z_i(t)$ —namely,  $r_i(t)$  and  $x_i(t)$ —are the inverse Fourier transforms of  $R_i(\omega) = \text{Re}\{Z_i(\omega)\}$  and of  $iX_i(\omega) = i\text{Im}\{Z_i(\omega)\}$ , respectively. Consequently, the inverse Fourier transform of  $Z_i^*(\omega)$  is

$$\mathcal{F}^{-1}\{Z_i^*(\omega)\} = r_i(t) - x_i(t) = r_i(-t) + x_i(-t) = z_i(-t). \quad (6.58)$$

Thus, whereas  $Z_i(\omega)$  corresponds to a causal impulse-response function  $z_i(t)$ , its conjugate  $Z_i^*(\omega)$  corresponds to a noncausal (and, in particular, an ‘anti-causal’) impulse-response function  $z_i(-t)$ , which vanishes for  $t > 0$ . Thus, apart from

exceptional cases (such as, e.g., when the incident wave is purely sinusoidal), the optimum condition (6.52) cannot be exactly satisfied in practice. Also, the optimum condition (6.55) cannot in general be realised exactly, because the transfer function  $R_i(\omega)$  or  $1/R_i(\omega)$  is even in  $\omega$  and consequently corresponds to an even (and, hence, noncausal) impulse-response function of time.

Moreover, also the transfer function  $f_e(\omega)$  corresponds to a noncausal impulse-response function  $f_t(t)$ , as explained in Subsection 5.3.2. Thus, three of the blocks shown in Figure 6.7 represent noncausal impulse-response functions, and consequently, they cannot be realised exactly. As an example, let us now discuss in some detail the relation  $F_e(\omega) = f_e(\omega)A(\omega)$  in the time domain. Using Eq. (5.111), we have for the excitation force

$$F_{e,t}(t) = \int_{-\infty}^{\infty} f_t(t - \tau) a(\tau) d\tau, \quad (6.59)$$

where  $f_t(t)$  and  $a(t)$  are the inverse Fourier transforms of  $f_e(\omega)$  and  $A(\omega)$ , respectively. Now, since  $f_t$  is noncausal—that is,  $f_t(t - \tau) \neq 0$  also for  $\tau > t$ —there is a finite contribution to the integral from the interval  $t < \tau < \infty$ . This means that future values of the incident wave elevation  $a(t)$  are required to compute the present-time excitation force  $F_{e,t}(t)$ . Similarly, since  $-Z_i^*(\omega)$  and  $1/R_i(\omega)$  represent noncausal impulse-response functions, future values of the actual body velocity  $u(t)$  and of the actual excitation force  $F_{e,t}(t)$  are needed to compute the present-time values of the optimum load force  $F_{u,t}(t)$  and the optimum body velocity  $u_t(t)$ , respectively.

Two different strategies may be attempted to solve these non-realisable (noncausal) optimum-control problems in an approximate manner. We may refer to these approximate strategies as suboptimal control methods. One strategy is to predict the relevant input quantities a certain time distance into the future, which is straightforward for purely sinusoidal waves and oscillations, and more difficult for a broad-band than for a narrow-band wave spectrum associated with a real-sea situation. The other strategy is to replace the transfer functions  $f_e(\omega)$ ,  $-Z_i^*(\omega)$  and  $1/2R_i(\omega)$  by practically realisable transfer functions, which represent causal impulse-response functions, and which approximate the ideal but non-realisable transfer functions. The aim is to make the approximation good at the frequencies which are important—that is, the interval of frequencies which contains most of the wave energy. Outside this interval, the chosen realisable transfer function may deviate very much from the corresponding ideal but non-realisable transfer function. With this version of a suboptimal strategy, too, better performance may be expected for a narrowband than for a broadband wave spectrum.

Several investigations have been carried out on future predictions of the wave elevation or hydrodynamic pressure at a certain point [40, 41] and also on the utilisation of future predictions for optimum wave-energy conversion [84, 85]. The method of replacing a non-realisable ideal transfer function by a realisable but suboptimal transfer function have also been investigated

to some extent [86–89]. The following paragraph, as an example, gives an outline of a causalising approximation, as proposed by Perdigão and Sarmento [86].

Let us discuss the approximation where the transfer function  $1/2R_i(\omega)$  in Eq. (6.55) has been replaced by a rational function  $N(\omega)/D(\omega)$ , where  $N(\omega)$  and  $D(\omega)$  are polynomials of order  $n$  and  $m$ , respectively. We want to ensure that the corresponding impulse-response function is causal and that the control is stable. For this reason, we impose the requirements that  $n < m$  and that  $D(\omega)$  has all its zeros in the upper half of the complex  $\omega$  plane. In accordance with this choice, we replace Eq. (6.55) with

$$u(\omega) = F_e(\omega)N(\omega)/D(\omega), \quad (6.60)$$

and a corresponding replacement may be made to change the appropriate non-realisable block in Figure 6.7 with a realisable one. Inserting Eq. (6.60) into Eq. (6.54) gives

$$\alpha(\omega) = |F_e(\omega)|^2 |1 - 2R_i(\omega)N(\omega)/D(\omega)|^2. \quad (6.61)$$

If this is inserted into the expression (6.47) for  $W_{u,P}$ , it becomes obvious that we, for a general  $F_e(\omega)$ , have  $W_{u,P} > 0$ . We now need to choose the unknown complex coefficients of the two polynomials in order to minimise  $W_{u,P}$ . For instance, if we had chosen  $m = 3$  and  $n = 2$ , that is,

$$\frac{N(\omega)}{D(\omega)} = \frac{b_0 + b_1\omega + b_2\omega^2}{1 + a_1\omega + a_2\omega^2 + a_3\omega^3}, \quad (6.62)$$

then six complex coefficients  $a_1$ ,  $a_2$ ,  $a_3$ ,  $b_0$ ,  $b_1$  and  $b_2$  need to be determined. Thus,  $W_{u,P}$  becomes a function of the unknown coefficients, which are determined such as to minimise  $W_{u,P}$  (observing the constraint that all zeros of  $D(\omega)$  have positive imaginary parts). We see that the wave spectrum, represented by the quantity  $|F_e(\omega)|^2$  in Eq. (6.61), will function as a weight factor in the integral (6.47), which is to be minimised. Hence, we expect the approximation to be good in the frequency interval where  $|F_e(\omega)|$  is large—in particular, if the wave spectrum is narrow. We observe that for a different wave spectrum—that is, for a different function  $F_e(\omega)$ —a new determination of the best polynomials  $N(\omega)$  and  $D(\omega)$  has to be made. Note, however, that we are not, in real time, able to determine the Fourier transform  $F_e(\omega)$  exactly, which would require integration over the interval  $-\infty < t < \infty$  [see Eq. (2.135)]. In practice, we have to determine  $F_e(\omega)$  only approximately based on measurement during the last minutes or hours.

## 6.4 The Budal Upper Bound (BUB)

Note from Eq. (6.12) that, when the velocity amplitude  $|\hat{u}_j| = |\hat{u}_j|_{OPT} = \omega|\hat{s}_j|_{OPT}$ , which is proportional to the elevation amplitude  $|A|$  of the incident wave, then

half of the incident excitation power  $P_e$  is absorbed while the remaining half is radiated, in order to produce the wave that is needed to interfere destructively with the incident wave. This may be the situation when the incident wave amplitude is rather low.

On the other hand, for larger wave amplitudes, the situation may be that  $|\hat{u}_j|_{\text{OPT}} \gg \omega|\hat{s}_j|_{\text{max}}$ , where  $|\hat{s}_j|_{\text{max}}$  is the design displacement amplitude of the WEC body. Then, since  $|\hat{u}_j| \ll |\hat{u}_j|_{\text{OPT}}$ , we have  $P_r \ll P \approx P_e$  (cf. Figure 6.3). That is, the excitation power is essentially absorbed by the WEC, and relatively little power is then radiated. However, in this case, only a small fraction of the wave power in the ocean is absorbed. Most of the wave power remains in the sea. Note that this situation, from an economic point of view, sometimes may be desirable for a WEC, particularly in situations with large wave heights. Because wave power in the ocean is free, whereas the realisation of a large body-velocity amplitude requires economical expenditure, it may be advantageous to aim at a design value of the velocity amplitude  $|\hat{u}_j| = \omega|\hat{s}_j|_{\text{max}}$  which is substantially smaller than  $|\hat{u}_j|_{\text{OPT}}$ , except during wave conditions when the wave amplitude  $|A|$  and, hence, also  $|\hat{F}_{ej}| = |f_{ej}A|$  and  $|\hat{u}_j|_{\text{OPT}}$  are rather small.

What should be maximised in practice is the ratio between the energy delivered by the WEC and the total cost including investment, maintenance and operation. However, it is a rather complicated and large task to provide a reliable information on this problem. A much simpler problem, studied four decades ago by Budal, is to consider the ratio between the absorbed power  $P$  and the volume  $V$  of a heaving semisubmerged WEC body. In the following, let us discuss an upper bound [83, 90] to this ratio. Firstly, however, we consider a few other upper bounds for the absorbed wave power  $P$ .

The converted useful power is at most equal to the absorbed power  $P$ . For the absorbed power, we have from Eqs. (6.4), (6.6) and (6.7) that

$$P < \frac{1}{2}|\hat{F}_{ej}| \cdot |\hat{u}_j| \cos \gamma_j \leq \frac{1}{2}|\hat{F}_{ej}| \cdot |\hat{u}_j|. \quad (6.63)$$

The two inequalities here approach equality if  $|\hat{u}_j| \ll |\hat{u}_j|_{\text{OPT}}$  and if the phase is approximately optimum, respectively.

For certain WEC bodies and modes, this design amplitude may be expressed as a simple function of the available hull volume  $V$ —for example,  $|\hat{s}_3|_{\text{max}} = V/2S_w$  for a heaving tall cylindrical body with water-plane area equaling  $S_w$ . In general, however, the design amplitude for an oscillating WEC body may be differently related to the size of the hull volume. The WEC body's useful oscillation amplitude may also be limited by, for example, the Keulegan–Carpenter number (see Section 6.4.4).

The design amplitude for an oscillating WEC body is somehow directly related to the volume of water displaced by the body. As explained earlier (for example, in Section 6.1), such an oscillating water-displacement volume is a necessity in order for the oscillating WEC body to absorb energy from an incident wave.

The excitation force amplitude is proportional to the wave amplitude  $|A|$  and is bounded by  $|f_{e,j}|_{\max} |A|$ . Thus, we have

$$|\hat{u}_j| \leq \omega |\hat{s}_j|_{\max} \quad \text{and} \quad |\hat{F}_{e,j}| \leq |f_{e,j}|_{\max} |A|. \quad (6.64)$$

Then, from Eq. (6.63), we have

$$P < P_K = c_K |s_j|_{\max} H/T, \quad (6.65)$$

where

$$c_K = \pi |f_{e,j}|_{\max}/2 \quad \text{and} \quad H = 2|A|. \quad (6.66)$$

In the present section, we are, in the mathematical sense, considering upper bounds rather than upper limits. Next, we shall discuss the Budal upper bound (BUB). As a preliminary, expressions (6.63) and (6.65) are considered to be examples of upper bounds—not upper limits (in the mathematical sense)—for the absorbed wave power. [To emphasise this, we remark that these two expressions are upper bounds for the absorbed wave power  $P$  even if we should wish to multiply the right-hand sides by any arbitrary factor that is larger than 1!]

Let us now assume that a semisubmerged body of volume  $V$  and water-plane area  $S_w$  is oscillating in heave. Thus, with  $j = 3$ , it is reasonable (at least for a body of cylindrical shape) to assume that the design amplitude  $|s_3|_{\max}$  for heave excursion does not exceed  $V/2S_w$ . Then we have the further inequalities

$$|\hat{u}_3| < \omega V/2S_w \quad \text{and} \quad |\hat{F}_{e,3}| < \rho g S_w |A|, \quad (6.67)$$

where we have made use of the small-body approximation (5.277). The latter inequality approaches equality if the horizontal extension of the body is very small compared to the wavelength. Combining inequalities (6.67) with the last of inequalities (6.63), we obtain

$$P < \frac{\rho g \omega V |A|}{4} = \frac{\pi \rho g V |A|}{2T} = \frac{\pi \rho g V H}{4T}, \quad (6.68)$$

where  $H = 2|A|$  is the wave height and  $T = 2\pi/\omega$  is the period of the wave as well as of the heave oscillation. Here, on the right-hand side,  $T$  and  $H$  are wave parameters, and the hull volume  $V$  is the only WEC-body parameter. Its size may perhaps serve as a rough indicator of parts of the investment cost of the WEC. We may expect that the simple inequality (6.68) has a larger right-hand side than inequalities (6.63) and (6.65). It might again be emphasised that these mathematical inequalities are upper bounds and not upper limits.

When deriving inequality (6.68), Budal [83, 90] considered a tall cylindrical body with a relatively small water-plane area. Then, with optimum phase ( $\gamma_3 = 0$ ), the heave amplitude  $|\hat{s}_3|$  may be significantly larger than the wave-elevation amplitude  $|A|$ . Inequalities (6.67) are based on this assumption. However, for a wave-interacting low cylindrical body with a relatively large water-plane area, the heave amplitude should not exceed the wave amplitude.

Moreover, the excitation force amplitude is bounded by the body's buoyancy force at equilibrium in still water. In this case, inequalities (6.67) are to be replaced with

$$|\hat{u}_3| < \omega|A| \quad \text{and} \quad |\hat{F}_{e,3}| < \rho g V/2, \quad (6.69)$$

as suggested by Rainey [91]. This alternative to inequalities (6.67) leads, however, to the same inequality (6.68).

Taking as typical values  $T = 8$  s and  $H = 2$  m, we find that inequality (6.68) gives an upper bound  $P/V < 2.0 \text{ kW/m}^3$ . From the preceding discussion, it becomes evident that to approach this upper bound, it is necessary that the body volume  $V$  tends to zero—which is, of course, not very practical for a WEC. However,  $V$  has to be as small as practical if we are to maximize the utilisation of the WEC body volume, which is what upper bound (6.68) is about. In Problem 6.2, we discuss a case of a heaving axisymmetric body of diameter  $2a = 6$  m, which is rather small compared to the 100 m wavelength for the considered 8 s wave. Although the body volume is as small as  $283 \text{ m}^3$ , we obtain in this case only  $0.8 \text{ kW/m}^3$  for  $P/V$ . This is significantly less than the upper bound  $2.0 \text{ kW/m}^3$ . A performance closer to this upper bound is, however, obtained with larger wavelengths and, thus, longer wave periods, as discussed in Problem 6.2.

It should be emphasised that inequality (6.68) was derived based on the assumption of sinusoidal wave and oscillation. With latching control, however, a larger upper bound is applicable [84]. Let us assume that the immersed body's vertical motion between its two extreme positions takes place momentarily at the instants of extreme heave force (cf. Figure 6.6). Then the heave position, as a function of time, corresponds to a periodic square-wave function, for which the first harmonic amplitude is a factor  $4/\pi \approx 1.27$  larger than its physical excursion from equilibrium.

Thus, assuming a sinusoidal wave, but only a periodic WEC-body motion, we may generalise the inequality (6.68) to

$$P < P_B = c_B VH/T, \quad (6.70)$$

where  $P_B$  is the *Budal upper bound (BUB)*. Further,

$$c_B = \sigma \rho g = \sigma \times 10.0 \times 10^3 \text{ W m}^{-4} \text{ s}, \quad (6.71)$$

where  $\rho = 1030 \text{ kg/m}^3$  is the mass density of seawater, and  $g = 9.81 \text{ m/s}^2$  is the acceleration of gravity. Moreover,

$$\sigma = \begin{cases} \sigma_s = \pi/4 & \text{for sinusoidal oscillation,} \\ \sigma_p = 1 & \text{for periodic oscillation.} \end{cases} \quad (6.72)$$

In both cases, a sinusoidal wave of period  $T = 2\pi/\omega$  and elevation amplitude  $|A| = H/2$  is assumed. For a typical case with  $T = 8$  s and  $H = 2$  m, we find an upper bound of  $P/V < 2.5 \text{ kW/m}^3$  for the case of periodic oscillation.

The Budal upper bound, given by Eq. (6.70), was derived by considering a heaving semisubmerged WEC body. As explained earlier, in Section 6.1, for an oscillating WEC body to absorb energy from an incident wave, it is required that the WEC body radiates a wave which interferes destructively with the incident wave. When the heaving, semisubmerged body of volume  $V$  moves downwards from its uppermost position to its lowest position, it pushes a volume of water  $V_{\text{water}} = V$  downwards and sideways. When it moves upwards, it sucks back an equally large amount of water. It is by this back-and-forth water motion that the WEC body is radiating the wave which is needed to remove energy from the incident wave. Thus, if we write

$$P < P_B = c_B V_{\text{water}} H/T, \quad (6.73)$$

then BUB is applicable also to certain other kinds of WECs, such as an OWC. These WECs are of the monopole-type of wave radiators/absorbers. When we have replaced the heaving-body volume  $V$  with the oscillating water volume  $V_{\text{water}}$ , the BUB in the form of inequality (6.73) becomes a universal upper bound.

We may understand this if we consider a dipole-type of wave radiator, such as an immersed thin horizontal cylinder performing surging oscillation in its axial direction. Let its vertical cross-sectional area be of a size equalling the horizontal cross-sectional area of the just considered heaving body. However, we let the surging, horizontal-axis cylinder be longer in the horizontal direction: we let the surging cylinder length be one-half of a wavelength. Thus, we may compare this surging cylinder to a set of two heaving, vertical-axis, cylindrical bodies, separated by half a wavelength in the direction of the incident-wave propagation. The size of displaced water amount  $V_{\text{water}}$  may, however, be larger for the surging WEC body than for the two heaving WEC bodies. The universal relationship (6.73), where the WEC body volume  $V$  has been replaced by the water volume amplitude  $V_{\text{water}}$ , is applicable in both cases. It is another manifestation of the principle that energy may be removed from an incoming wave by radiating a wave that interferes destructively with it. To radiate a wave, the WEC body needs to alternately push and suck a certain amount of water during each oscillation cycle.

#### 6.4.1 Two Different Upper Bounds for Absorbed Power

The BUB inequality (6.70) represents an upper bound for the wave power which may be absorbed from a sinusoidal wave by a heaving semisubmerged body. Observe that the BUB is an *upper bound*, and not, in the mathematical sense, an upper limit.

In contrast, according to Eq. (6.13), another upper bound,  $P \leq P_A = G(\beta)J/k$ , which is valid for constant water depth  $h$ , may, in certain ideal cases, even correspond to an upper limit. For the mathematically simpler case of deep water, this upper-bound relationship may, according to Eq. (6.16), be simplified to

$$P \leq P_A = c_A H^2 T^3. \quad (6.74)$$

The coefficient  $c_A = c_{A,j}$  is given by Eq. (6.17) for each of the WEC body's oscillation modes,  $j = 1, \dots, 6$ . In the following, discussing an axisymmetric body in the heave mode, we shall, for convenience, omit the subscript  $j = 3$ . Then, since  $G_3(\beta) \equiv 1$ ,

$$c_A = c_{A,3} = \rho(g/\pi)^3/128 = 245 \text{W m}^{-2}\text{s}^{-3}, \quad (6.75)$$

according to Eq. (6.17).

Note that this latter upper bound, inequality (6.74), depends on the WEC body's shape and oscillation mode, but not on its size. It corresponds to an ideal situation where the available sea-wave energy is exploited as much as possible. On the other hand, the BUB, inequality (6.70), as well as its generalisations (6.73) and (6.65), concerns an optimum utilisation of the deployed WEC hull size, or maximum stroke. We may call inequality (6.74) theoretical upper bound and inequality (6.70), (6.73) or (6.65) practical upper bound. For wave periods  $T \leq T_c$ , for example, upper bound (6.74) governs, whereas for  $T \geq T_c$ , upper bound (6.70), (6.73) or (6.65) governs. A WEC should exploit the available wave energy as much as possible for  $T \leq T_c$ , since at these periods the hull size or maximum stroke is not a restriction. On the other hand, a WEC should utilise its hull size or design stroke as much as possible for  $T \geq T_c$ , because at these periods, these limits govern the maximum energy that can practically be absorbed by the WEC.

Notice that the dependence on the wave period  $T$  is very much different in the two upper bounds. The power of  $T^{-1}$  in BUB reflects the fact that the WEC body performs more oscillation strokes per hour for shorter wave periods, while the power of  $T^3$  in Eq. (6.74) reflects the fact that with increasing  $T$ , firstly, the wave motion extends more deeply below the sea surface and, secondly, the group velocity is larger.

Based on the two upper bounds and on wave data for a particular ocean site, we shall, in the following, make a reasonable decision upon sizes of PTO capacity and of WEC hull volume for a simple axisymmetric example. The two upper-bound relations (6.70) and (6.74) and also some additional upper-bound relations for WECs have during recent years been discussed in more detail in several papers [77, 92, 93].

#### 6.4.2 Axisymmetrically Radiating WEC Body

For a WEC body radiating isotropically, the two different upper-bound curves, one monotonically ascending curve for  $P_A$  and one monotonically descending curve for  $P_B$ , are illustrated in the  $P$ -versus- $T$  diagram of Figure 6.10—for example, where  $V = 524 \text{m}^3$  and  $H = 2.26 \text{m}$ . The two curves intersect at a point  $(T_c, P_c) = (T_{c,s}, P_{c,s}) = (9.3 \text{s}, 1.0 \text{MW})$ , for which  $P_A = P_B \equiv P_c$ . From Eqs. (6.70) and (6.74), we now find the intersection-point relations

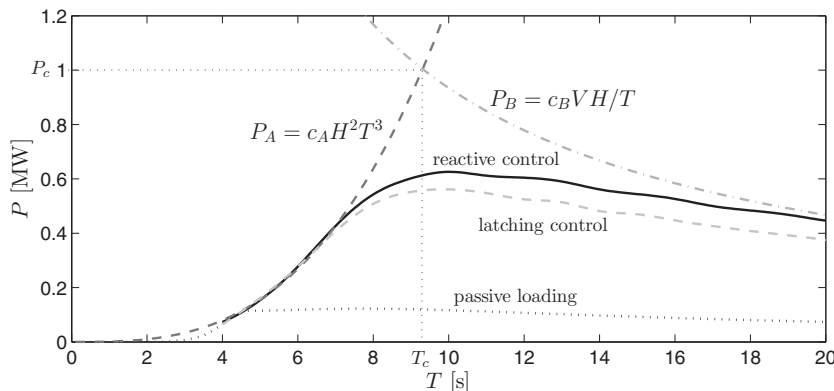


Figure 6.10: The two upper, monotonically increasing and decreasing curves show, according to Eqs. (6.74) and (6.70), two different upper bounds— $P_A$  and  $P_B$ , respectively—for the maximum possible power  $P$  which may be absorbed from a sinusoidal wave of height  $H$  and period  $T$  by means of an immersed heaving axisymmetric WEC of volume stroke  $V$ . The shown scales for  $T$  and  $P$  are applicable when  $H = 2.26$  m,  $V = 524$  m $^3$  and  $\sigma = \pi/4$ . The two curves' intersection point is  $(T_c, P_c) = (T_{cs}, P_{cs}) = (9.3$  s,  $1.0$  MW), as indicated by two straight dotted lines. Below the two upper-bound curves for  $P_A$  and  $P_B$ , three numerically computed theoretical curves are shown, where it has been assumed that the WEC is a semisubmerged sphere, which is heaving with optimum amplitude, but with three different phase-control methods, as indicated on the diagram. The sphere has a diameter of  $2a = 10$  m, and its heave amplitude is load-constrained to not exceed 3 m. (The figure is a variant of figure 6 in [77]).

$$T_c^4 = \frac{c_B V}{c_A H} \quad \text{and} \quad P_c^4 = c_A c_B^3 V^5 H^3. \quad (6.76)$$

Thus, the ‘WEC parameters’  $P_c$  and  $V$  can be expressed in terms of ‘wave parameters’  $H$  and  $T_c$  as

$$P_c = c_A H^2 T_c^3 = (245 \text{ W m}^{-2} \text{ s}^{-3}) H^2 T_{cs}^3, \quad (6.77)$$

$$V = (c_A/c_B) H T_c^4 = (0.0310 \text{ W m}^2 \text{ s}^{-4}) H T_{cs}^4, \quad (6.78)$$

where  $\sigma = \sigma_s = \pi/4$  is implied with the numerical value of the intersection-point wave period  $T_{cs}$ ; cf. Eqs. (6.72).

Below these two upper-bound curves, Figure 6.10 contains three curves, which represent computed values for the wave power absorbed by the heaving WEC body, assumed to be a semisubmerged sphere of diameter  $2a = 10$  m and volume  $V = 524$  m $^3$ . These three curves—corresponding to reactive control, latching control and passive operation—show maxima significantly below the intersection-point power  $P_c$ . The passive-loading curve touches the  $P_A$  curve at the heave-resonance period  $T \approx 4.3$  s. The reactive-control curve follows the  $P_A$  curve from the same resonance period 4.3 s to a period about 6.8 s, where  $P_B > 2P_A$ . For the wave height  $H$  in question, the  $P_A$  curve is unreachable when  $P_B < 2P_A$ .

For reactive control and for latching control, the oscillation is not sinusoidal. Thus, for these two cases, the BUB with  $\sigma = \sigma_u = 1$  is applicable. This is

not shown in Figure 6.10, but it would correspond to an intersection point  $(T_c, P_c) = (T_{c,u}, P_{c,u}) = (9.9 \text{ s}, 1.2 \text{ MW})$ . Looking at the right-hand portions of the two curves corresponding to reactive control and latching control in Figure 6.10, one might expect that they, if extrapolated to larger wave periods, may extend above the shown monotonically declining BUB curve, corresponding to  $\sigma = \sigma_s = \pi/4$ .

Based on a diagram shown in Figure 6.10 and several other similar diagrams [77, 92, 93], it may be concluded that the *maximum* absorbed wave power  $P_{\max}$  relative to the intersection-point power  $P_{c,s}$  is roughly only a fraction of about

$$P_{\max}/P_{c,s} \approx \begin{cases} 0.6 & \text{for reactive control} \\ 0.5 & \text{for latching control} \\ 0.1 & \text{for passive system,} \end{cases} \quad (6.79)$$

corresponding to power takeoff (PTO) capacity of 0.6 MW, 0.5 MW or 0.1 MW respectively.

For a wave period of  $T = 8 \text{ s}$ , the chosen wave height  $H = 2.26 \text{ m}$  has a rather high probability of occurrence off the European Atlantic coast but a significantly less probability for wave periods above 10 s. Thus, it may be favorable to choose a much smaller—and hence less expensive—WEC body than the present one, for which the diameter is 10 m. This would also lower both intersection-point values  $T_c$  and  $P_c$ . The WEC unit may then be better matched to our oceans' wave climate.

According to definitions in Section 6.1.1, this heaving 10 m diameter WEC body is a quasi-point absorber (QPA) for wavelengths  $\lambda < 200 \text{ m}$ —that is, for wave periods  $T < 11 \text{ s}$  and, thus, for the substantial part of our oceans' wind-generated wave energy. Next, we consider a significantly smaller WEC body, designed for converting energy from waves of periods in the range of 6 to 11 s.

### 6.4.3 A Point Absorber

North Atlantic wave data off the west coast of Scotland [94, p. 80] indicate that the wave-power level  $J$  exceeds about 40 kW/m during about one-third of the year. Thus, it is reasonable to base the design of a WEC body on this level. Moreover, it appears that wave states occur rather rarely outside the wave-period region from 6 s to 11 s and most frequently for wave periods  $T$  within the interval  $7 \text{ s} < T < 9 \text{ s}$ .

Observing the absorbed-power curves on Figure 6.10, we note that the response stays high in a much wider wave-period range above rather than below the intersection wave period  $T_c$ . For this reason, we shall choose an intersection-point period significantly below 8 s. Then the BUB curve for  $P_B$  in the diagram of Figure 6.10 has to be lowered, corresponding to a smaller WEC-body volume  $V$ . In this  $P$ -versus- $T$  diagram, the wave height  $H$  and the WEC-body volume  $V$  are constant, given parameters. If the volume is reduced, the  $P_B$  curve is lowered

in the same proportion, but the  $P_A$  curve remains unchanged. The intersection point  $(T_c, P_c)$  will slide down along this  $P_A$  curve. The immersed WEC body volume is better utilised, but less energy will be removed from the sea waves by each WEC unit. Thus, if many smaller WEC bodies are deployed in a WEC array, the distance between adjacent WEC-body units may need to be shorter.

As an example, let us consider a single WEC body which is a heaving semisubmerged vertical cylinder of radius  $a$  and height  $b$ . As argued later, in Section 6.4.4, we shall choose  $b \geq 2a$ . Let us assume that its diameter is  $2a = 5$  m. Then, the cylindrical WEC body has a volume of  $V' = \pi a^2 b \geq 2\pi a^3 = 98$  m<sup>3</sup>. It is a point absorber (PA) for wavelengths  $\lambda > 20 \times 2a = 100$  m; thus, according to Eq. (4.100), for wave periods  $T > 8.0$  s. Otherwise, for smaller wave periods, it will be a QPA.

Because of the smaller volume  $V'$  (here assumed to be 98 m<sup>3</sup>), the intersection point corresponds to smaller values  $(T'_c, P'_c) = (T'_{c,s}, P'_{c,s}) = (6.1$  s, 0.29 MW), as obtained from the two equations (6.76). The coarse approximations (6.79) concerning a WEC's PTO capacity are presumably still valid. Correspondingly, if each WEC unit is equipped for optimum-control operation, then its PTO capacity should be about 0.15 MW.

The vertical cylindrical body should, at its lower end, be extended with a hemisphere, of the same diameter  $2a = 5$  m. The main purpose is to reduce the risk of energy loss from the shedding of vortices. (See the following Section 6.4.4.) An additional purpose is to provide the possibility of lowering the WEC body's centre of gravity. The intended maximum heave amplitude is  $b$ , and the equilibrium draft of the axisymmetric WEC body is then  $a + b$ .

#### 6.4.4 Importance of the Keulegan–Carpenter Number

Figure 6.1(b) may serve as an illustration of the 5 m diameter WEC body considered in Section 6.4.3 when downscaled and tested in a wave channel.

If such a reduced-size laboratory model has a diameter of  $2a = 150$  mm, the length scale is  $1 : 33.3$ . Then the time scale is  $1 : \sqrt{33.3} = 1 : 5.77$ , because the acceleration of gravity is  $g = 9.81$  m/s<sup>2</sup> in model scale as well as in full scale. The volume scale is  $1 : 33.3^3 = 1 : 37.0 \times 10^3$ , as is also the force scale if we neglect the difference between sea-water and fresh-water mass densities. Then the energy scale is  $1 : 33.3^4 = 1 : 1.23 \times 10^6$ , and the power scale is  $1 : 33.3^{7/2} = 1 : 214 \times 10^3$ .

Such a laboratory model has been arranged to realise resonant heave oscillation of wave period  $T = 1.49$  s, corresponding to full-scale period  $T = 8.6$  s. The width of the wave channel is 0.50 m, and the water depth is  $h = 1.50$  m. Thus, according to Eq. (4.54), the wavelength is  $\lambda = 3.4$  m, corresponding to a full-scale value of 115 m. As the diameter is  $2a < \lambda/20$ , the model may be classified as a point absorber in the performed model experiments [95].

An important part of these laboratory experiments is the linearity tests, with results as shown in Figure 6.11, where the horizontal scale shows wave amplitude, while the vertical scale shows heave amplitude, under conditions when the

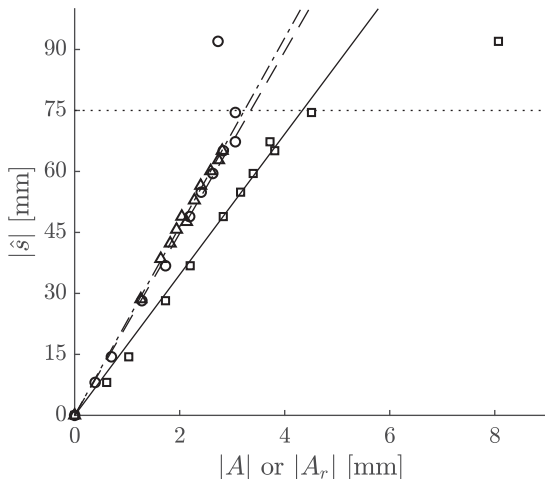


Figure 6.11: Heave oscillation versus wave elevation. Three sets of linearity tests on a heaving vertical, 150 mm diameter cylinder, which is extended with a hemisphere on its lower end. It is immersed to an equilibrium draft of  $(100 + 75) \text{ mm} = 0.175 \text{ m}$ , in a 0.50 m wide wave channel, where the water depth is  $h = 1.50 \text{ m}$ . Sinusoidal oscillations have a period of  $T = 1.49 \text{ s}$ . Square plots show resonant heave amplitude  $|\dot{s}|$  responding to incident-wave amplitude  $|A| = H/2$ , when the mechanical load is minimised to include only unavoidable friction and viscosity losses. Triangular plots show radiated wave amplitude responding to the body's heave amplitude when there is no incident wave. Circular plots show the radiated wave amplitude  $|A_r|$  responding to the body's heave amplitude  $|\dot{s}|$  caused by the incident-wave amplitude  $|A|$ . Note that then an almost negligible diffracted-wave contribution is included in this  $|A_r|$ . The dotted horizontal line indicates where the Keulegan-Carpenter number equals  $\pi$ . The inclined straight lines through the origin are matched to the experimental points, excluding points for which  $|\dot{s}| > 70 \text{ mm}$ . These three lines have steepnesses 23, 22 and 17. (This figure is a variant of figure 4 in [95])

damping load of oscillation is minimised to include only unavoidable viscosity and friction losses. Three inclined straight lines of steepnesses 17, 22 and 23 are matched to the experimental points for which the heave amplitude is less than 70 mm. The lines with steepnesses 17 and 22 correspond to the right-hand zero crossing of the lower and upper parabola, respectively, as shown in Figure 6.3.

The experimental results shown by square plots in Figure 6.11 show the body's heave amplitude  $|\dot{s}|$  resulting from a sinusoidal wave of amplitude  $|A|$  propagating along the wave flume. Deviation from linearity indicates that the wave's ability to move the immersed body is seriously impoverished if the heave amplitude exceeds 75 mm, which here equals the minimum radius of curvature of the immersed WEC-body surface. This demonstrates that for oscillatory flow it may be very important to consider the Keulegan-Carpenter number  $N_{KC}$ .

We suggest that numerical oscillating-fluid results based on potential theory may be applicable if the *relative* oscillation amplitude  $|\dot{s}_b|$  of the water, along the immersed WEC-body surface, nowhere exceeds the local radius of curvature  $\rho_b$  on this surface. Then the Keulegan-Carpenter number [96]

$$N_{KC} \equiv \pi |\hat{v}_b| / (\omega \rho_b) = \pi |\hat{s}_b| / \rho_b < \pi \quad (6.80)$$

is small enough for avoidance of vortex shedding and corresponding energy loss. Here  $|\hat{v}_b|$  is the tangential relative water velocity along the WEC-body's wet surface at its minimum radius of curvature,  $\rho_b$ . This number is related to possible loss of energy related to the occurrence of vortices being shed from the oscillating body. A lesson to learn is that sharp edges or corners on a WEC body's wet surface should be avoided.

While the square plots in Figure 6.11 show the primary heave response caused by the incident wave, a secondary response is a radiated wave—including an almost negligible diffracted-wave contribution—as shown by the circular plots. Note that, in this case, when the Keulegan–Carpenter number approaches, or exceeds  $\pi$ , the oscillating body reduces its ability both to radiate a wave and to convert wave energy. Remember Budal's formulation: to absorb a wave means to radiate a wave!

Concerning the triangular plots in Figure 6.11, there is no diffracted-wave contribution but only a radiated wave. The waves were generated by exciting the body to oscillate, while the wave channel's own wavemaker was not used. Thus, for these triangular plots, there is only a radiated wave without any diffracted-wave contribution.

## 6.5 Several WEC-Body Modes

As discussed in Section 5.1, an immersed body may oscillate in up to six different modes  $j$  ( $j = 1, 2, \dots, 6$ ). Moreover, if there is an incident wave, an excitation force  $F_{ej}$  results, as discussed also in Sections 5.5.1 and 5.5.5. As a response to the excitation force, the immersed body may attain a velocity  $u_j$  whereby an additional wave force, the radiation force,  $F_{r,j}$ , is set up. In accordance with Eq. (5.155), the total wave force in oscillating mode  $j$  has a complex amplitude

$$\hat{F}_{t,j} = \hat{F}_{ej} + \hat{F}_{r,j} = f_j(\beta)A - \sum_{j'=1}^6 Z_{jj'}\hat{u}_{j'} \quad (6.81)$$

where  $Z_{jj'}$  is an element of the radiation impedance matrix, which is discussed in Sections 5.2.1, 5.5.1 and 5.5.3. Further,  $\beta$  is the angle of wave incidence, and  $A$  is the complex wave-elevation amplitude of the undisturbed incident wave at the chosen sea-surface reference point for the immersed WEC body. In accordance with Eq. (2.76), the (time-average) power absorbed by oscillating mode  $j$  is

$$P_j = \frac{1}{2} \operatorname{Re}\{\hat{F}_{t,j}\hat{u}_j^*\} = \frac{1}{4} (\hat{F}_{t,j}\hat{u}_j^* + \hat{F}_{t,j}^*\hat{u}_j), \quad (6.82)$$

which, in view of Eq. (6.81), may be written as

$$P_j = \frac{1}{4} [f_j(\beta)A\hat{u}_j^* + f_j^*(\beta)A^*\hat{u}_j] - \frac{1}{4} \sum_{j'=1}^6 (Z_{jj'}\hat{u}_{j'}\hat{u}_j^* + Z_{jj'}^*\hat{u}_{j'}^*\hat{u}_j). \quad (6.83)$$

By application of Eq. (5.24)—see also Section 2.3.1—we find the (time-average) power absorbed by the oscillating body:

$$P = \sum_{j=1}^6 P_j = P_e - P_r \equiv AE(\beta) + A^*E^*(\beta) - |U|^2, \quad (6.84)$$

where we have generalised the one-mode quantities  $E(\beta)$  and  $U$  introduced in Section 6.2.3. Here,

$$P_e = \frac{1}{4} \sum_{j=1}^6 (\hat{F}_{ej}\hat{u}_j^* + \hat{F}_{ej}^*\hat{u}_j) = \frac{1}{4} (\hat{\mathbf{F}}_e^T \hat{\mathbf{u}}^* + \hat{\mathbf{F}}_e^\dagger \hat{\mathbf{u}}) = AE(\beta) + A^*E^*(\beta) \quad (6.85)$$

is the excitation power. (Note that we may, if we wish, replace  $\hat{\mathbf{F}}_e^\dagger \hat{\mathbf{u}}$  with  $\hat{\mathbf{u}}^T \hat{\mathbf{F}}_e^*$ .) Moreover,

$$P_r = \frac{1}{2} \sum_{j=1}^6 \sum_{j'=1}^6 R_{jj'} \hat{u}_{j'} \hat{u}_j^* = \frac{1}{2} \hat{\mathbf{u}}^\dagger \mathbf{R} \hat{\mathbf{u}} = \frac{1}{2} \hat{\mathbf{u}}^T \mathbf{R} \hat{\mathbf{u}}^* \equiv |U|^2 \quad (6.86)$$

is the radiated power.

Here we have generalised to a six-mode case the two, complex, collective scalar parameters, the *collective excitation-power coefficient*  $E(\beta)$  and the *collective oscillation amplitude*  $U$ , which are introduced in Section 6.2.3, for a single-mode case. These results may be extended, not only to a six-mode WEC body, but even to an array of WEC bodies, as shown in more detail in Section 8.1. Comparison of Eqs. (6.32) and (6.84) demonstrates that the *wave-power ‘island’* (cf. Figure 6.5) is applicable even for a WEC body oscillating in up to six different modes [63].

In Eqs. (6.85) and (6.86), we have applied the matrix notation introduced in Chapter 5. When deriving Eq. (6.86), we have utilised the fact that the radiation resistance matrix  $\mathbf{R}$  is real and symmetric. Moreover, we have made use of the reciprocity relationship (5.175) and also Eq. (5.176), from which it follows that

$$\frac{1}{4}(Z_{jj'} + Z_{j'j}^*) = \frac{1}{4}(Z_{jj'} + Z_{jj'}^*) = \frac{1}{2}R_{jj'}. \quad (6.87)$$

Assuming that all  $\hat{F}_{ej}$  and all  $\hat{u}_j$  are known, the total absorbed power  $P$  is given by Eqs. (6.84)–(6.86), provided that all matrix elements  $R_{jj'}$  are also known. It is not necessary to know the imaginary part of the radiation impedance matrix. However, in order to determine the partition of absorbed power among the six individual oscillating modes, Eq. (6.83) shows that knowledge of the imaginary part of all  $Z_{jj'}$ , or, thus, of the added-mass matrix, is also required. This knowledge is also necessary in order to find from Eq. (6.81) the total wave force  $\hat{F}_{tj}$  in oscillating mode  $j$ .

As shown in the following, the last term in Eq. (6.84), the radiated power  $P_r$ , is necessarily nonnegative. Thus, it is possible for it to be represented as the modulus square of some complex quantity  $U$ . The argument is as follows.

In the case of no incident wave ( $A = 0$ ), we have  $F_{e,j} \equiv 0$  and, hence,  $P_e = 0$ . If, in spite of this, the immersed body oscillates (due to external forcing), it would work as a wave generator (that means  $P < 0$ ), except in particular cases when an immersed body may oscillate in an ideal fluid without the existence of any nonzero radiated wave in the far-field region (in these cases,  $P = 0$ , which is possible only if the radiation resistance matrix is singular). In this situation, it is impossible to have a positive absorbed power  $P$ . Otherwise, the principle of conservation of energy would be violated. Equation (6.84) then tells us that  $P_r \geq 0$  or, in view of Eq. (6.86),

$$\hat{\mathbf{u}}^\dagger \mathbf{R} \hat{\mathbf{u}} \geq 0 \quad (6.88)$$

for all possible values of  $\hat{\mathbf{u}}$ . Thus, according to this inequality, the radiation resistance matrix  $\mathbf{R}$  is positive semidefinite [16, p. 50], since  $\mathbf{R}$  is a real symmetric matrix ( $\mathbf{R}^\dagger = \mathbf{R}^T = \mathbf{R} = \mathbf{R}^*$ ). If  $\mathbf{R}$  is a non-singular matrix, it is positive definite. However, in many cases, as we have seen in Sections 5.7 and 5.8, the radiation resistance matrix is singular (its rank is less than its order.) For instance, with a general axisymmetric body, it is possible to choose nonzero complex velocity amplitudes for the surge and pitch modes in such a way that, by mutual cancellation, the resulting radiated wave vanishes. Hence, in the general case, we may only state that the matrix is positive semidefinite. Thus, because Eq. (6.88) holds, it is possible to state that the left-hand side of Eq. (6.86) is equal to the modulus square of a certain complex quantity  $U$ .

So far, we have no requirement on the arbitrary phase (argument) of the complex quantity  $U$ . We shall, however, find it convenient to let it have the same phase as  $A^* E^*(\beta)$  appearing in Eq. (6.84). Then  $A^* E^*(\beta)/U$  is a real positive quantity, which is, notably, independent of the complex velocity amplitude  $\hat{\mathbf{u}}$ . This means that, for example, Eq. (6.37) is applicable even for this six-mode WEC body.

### 6.5.1 Maximum Absorbed Power and Useful Power

Let us now consider the situation in which the incident wave has a relatively small amplitude, while there is no constraint on how to choose the complex velocity amplitudes  $\hat{u}_j$  for the body's oscillating modes. We wish to determine these amplitudes so that the absorbed power  $P$  becomes a maximum. To this end, we define the column vector

$$\boldsymbol{\delta} = \hat{\mathbf{u}} - \mathbf{U}, \quad (6.89)$$

where  $\mathbf{U}$  is a solution of the linear algebraic equation

$$\mathbf{R}\mathbf{U} = \frac{1}{2}\hat{\mathbf{F}}_e. \quad (6.90)$$

We now utilise the fact that  $\mathbf{R}$  is a matrix which is real and symmetric. Thus, the transpose of Eq. (6.90) is  $\hat{\mathbf{F}}_e^T/2 = \mathbf{U}^T \mathbf{R}^T = \mathbf{U}^T \mathbf{R}$ . Inserting  $\hat{\mathbf{u}} = \mathbf{U} + \boldsymbol{\delta}$  into Eqs. (6.85) and (6.86), we obtain from Eq. (6.84)

$$\begin{aligned}
P = P(\hat{\mathbf{u}}) &\equiv \frac{1}{4}(\hat{\mathbf{F}}_e^T \hat{\mathbf{u}}^* + \hat{\mathbf{F}}_e^\dagger \hat{\mathbf{u}}) - \frac{1}{2}\hat{\mathbf{u}}^\dagger \mathbf{R}\hat{\mathbf{u}} \\
&= \frac{1}{4}\hat{\mathbf{F}}_e^T \mathbf{U}^* + \frac{1}{4}\hat{\mathbf{F}}_e^\dagger \mathbf{U} + \frac{1}{4}\hat{\mathbf{F}}_e^T \boldsymbol{\delta}^* + \frac{1}{4}\hat{\mathbf{F}}_e^\dagger \boldsymbol{\delta} \\
&\quad - \frac{1}{2}\mathbf{U}^\dagger \mathbf{R}\mathbf{U} - \frac{1}{2}\boldsymbol{\delta}^\dagger \mathbf{R}\mathbf{U} - \frac{1}{2}\mathbf{U}^\dagger \mathbf{R}\boldsymbol{\delta} - \frac{1}{2}\boldsymbol{\delta}^\dagger \mathbf{R}\boldsymbol{\delta}.
\end{aligned} \tag{6.91}$$

Of these eight terms, only the first and eighth terms remain after mutual cancellation among the other terms. Since all terms are scalars, they equal their transposes. By transposing the third term, we see that it is cancelled by the sixth term after utilising Eq. (6.90). Applying the transposed conjugate of Eq. (6.90) in the seventh term, we see that it cancels the fourth term, and similarly, the second and the fifth terms cancel each other. Hence,

$$P = P(\hat{\mathbf{u}}) = P(\mathbf{U} + \boldsymbol{\delta}) = \frac{1}{4}\hat{\mathbf{F}}_e^T \mathbf{U}^* - \frac{1}{2}\boldsymbol{\delta}^\dagger \mathbf{R}\boldsymbol{\delta}. \tag{6.92}$$

So far, this is just another version of Eqs. (6.84)–(6.86). However, observing inequality (6.88), which means that  $\mathbf{R}$  is positive semidefinite, we see that the maximum absorbed power is

$$P_{\text{MAX}} = P(\mathbf{U}) = \frac{1}{4}\hat{\mathbf{F}}_e^T \mathbf{U}^*, \tag{6.93}$$

since the last term in Eq. (6.92) can only reduce, and not increase,  $P$ .

If the radiation resistance matrix  $\mathbf{R}$  is non-singular, its inverse  $\mathbf{R}^{-1}$  exists and Eq. (6.90) has a unique solution for the optimum velocity:

$$\hat{\mathbf{u}}_{\text{OPT}} \equiv \mathbf{U} = \frac{1}{2}\mathbf{R}^{-1}\hat{\mathbf{F}}_e. \tag{6.94}$$

Then only  $\boldsymbol{\delta} = 0$  can maximise Eq. (6.92). If  $\mathbf{R}$  is singular, the algebraic equation (6.90) is indeterminate. We know that then the last term in Eq. (6.92) can vanish for some particular non-vanishing values of  $\boldsymbol{\delta}$ . (See, for instance, Section 5.7.2.) Adding such a  $\boldsymbol{\delta}$  to  $\mathbf{U}$ , we obtain another optimum velocity  $\boldsymbol{\delta} + \mathbf{U}$ , which gives the same maximum absorbed power as given by Eq. (6.93). Thus, even though the optimum velocity  $\hat{\mathbf{u}}_{\text{OPT}}$  is ambiguous when  $\mathbf{R}$  is singular, the maximum absorbed power is unique. This maximum necessarily results if the velocity is given as one of the possible solutions of Eq. (6.90) (also see Problem 8.3.)

Because  $P_{\text{MAX}}$  is real and scalar, we may transpose and conjugate the right-hand side of Eq. (6.93). If we also use Eqs. (6.85), (6.86) and (6.90), we may choose among several expressions for the maximum absorbed power, such as

$$P_{\text{MAX}} = P_{r,\text{OPT}} = \frac{1}{2}P_{e,\text{OPT}} = \frac{1}{2}\hat{\mathbf{u}}_{\text{OPT}}^T \mathbf{R}\hat{\mathbf{u}}_{\text{OPT}}^* = \frac{1}{4}\hat{\mathbf{F}}_e^T \hat{\mathbf{u}}_{\text{OPT}}^* = \frac{1}{4}\hat{\mathbf{u}}_{\text{OPT}}^T \hat{\mathbf{F}}_e^* = |U_0|^2. \tag{6.95}$$

If  $\mathbf{R}$  is non-singular, it is also possible to use Eq. (6.94) to obtain

$$P_{\text{MAX}} = \frac{1}{8}\hat{\mathbf{F}}_e^T \mathbf{R}^{-1}\hat{\mathbf{F}}_e^* = \frac{1}{8}\hat{\mathbf{F}}_e^\dagger \mathbf{R}^{-1}\hat{\mathbf{F}}_e. \tag{6.96}$$

We now take into consideration energy loss due to friction and viscosity, by applying the simplified modelling proposed in Section 5.9. In analogy with Eq. (6.86) for the radiated power, the lost power is

$$P_{\text{loss}} = \frac{1}{2} \hat{\mathbf{u}}^T \mathbf{R}_f \hat{\mathbf{u}}^*, \quad (6.97)$$

where  $\mathbf{R}_f$  is the friction resistance matrix introduced in Eq. (5.340). The difference between the absorbed power and lost power is

$$P_u = P - P_{\text{loss}} = P_e - P_r - P_{\text{loss}}, \quad (6.98)$$

which we shall call useful power. Using Eqs. (6.85), (6.86) and (6.97), we get

$$P_u = \frac{1}{4} (\hat{\mathbf{F}}_e^T \hat{\mathbf{u}}^* + \hat{\mathbf{F}}_e^\dagger \hat{\mathbf{u}}) - \frac{1}{2} \hat{\mathbf{u}}^T (\mathbf{R} + \mathbf{R}_f) \hat{\mathbf{u}}^*. \quad (6.99)$$

If in Eq. (6.90) we replace  $\mathbf{R}$  with  $(\mathbf{R} + \mathbf{R}_f)$ , we get the optimum condition for the oscillation velocities which maximise the useful power. If we use these optimum velocities in Eq. (6.95) and also replace  $\mathbf{R}$  by  $(\mathbf{R} + \mathbf{R}_f)$ , we obtain the maximum useful power. Even though  $\mathbf{R}$  is in many cases a singular matrix, we expect that  $\mathbf{R} + \mathbf{R}_f$  is usually non-singular. Then we have the maximum useful power

$$P_{u,\text{MAX}} = \frac{1}{8} \hat{\mathbf{F}}_e^\dagger (\mathbf{R} + \mathbf{R}_f)^{-1} \hat{\mathbf{F}}_e^* \quad (6.100)$$

and the corresponding vector

$$\hat{\mathbf{u}} = \frac{1}{2} (\mathbf{R} + \mathbf{R}_f)^{-1} \hat{\mathbf{F}}_e \quad (6.101)$$

for the optimum complex velocity-amplitude components.

Due to the off-diagonal elements of the radiation resistance matrix  $\mathbf{R}$ , condition (6.90) or (6.101) for the optimum tells us that, for mode number  $i$ , it is not necessarily the best, in the multi-mode case, to have the velocity  $u_i$  in phase with the excitation force  $F_{e,i}$ .

## 6.5.2 Axisymmetric WEC Body

Let us now consider some examples of maximum power absorption with no constraints on the amplitudes.

With heave motion as the only mode of oscillation for a single axisymmetric body, the radiation resistance matrix  $\mathbf{R}$  and the excitation force vector  $\hat{\mathbf{F}}_e$  are simplified to the scalars  $R_{33}$  and  $F_{e,3} = f_{30}A$ , respectively. Then we have, according to Eqs. (6.94) and (6.96) [see also Eq. (3.45)],

$$P_{\text{MAX}} = \frac{|\hat{F}_{e,3}|^2}{8R_{33}} \quad \text{when} \quad \hat{u}_3 = \hat{u}_{3,\text{OPT}} = \frac{\hat{F}_{e,3}}{2R_{33}}. \quad (6.102)$$

Using Eqs. (4.130) and (5.302) gives

$$P_{\text{MAX}} = \frac{|f_3|^2}{8R_{33}} |A|^2 = \frac{|f_{30}|^2}{8R_{33}} |A|^2 = \frac{2\rho g^2 D(kh)}{8\omega k} |A|^2 = \frac{\rho g v_g}{2k} |A|^2 = \frac{1}{k} J, \quad (6.103)$$

where  $J$  is the incident wave power transport per unit frontage of the incident wave. Thus, the maximum absorption width is

$$d_{a,\text{MAX}} = \frac{P_{\text{MAX}}}{J} = \frac{1}{k} = \frac{\lambda}{2\pi}. \quad (6.104)$$

This result was first derived independently by Newman [34], Budal and Falnes [70] and Evans [75].

Next let us consider the case of a single axisymmetric body oscillating in just the three translational modes: surge, sway and heave. The oscillation velocity components, the excitation force components and the radiation resistance matrix may be written as

$$\hat{\mathbf{u}} = \begin{bmatrix} \hat{u}_1 \\ \hat{u}_2 \\ \hat{u}_3 \end{bmatrix}, \quad \hat{\mathbf{F}}_e = \begin{bmatrix} \hat{F}_{e,1} \\ \hat{F}_{e,2} \\ \hat{F}_{e,3} \end{bmatrix}, \quad \mathbf{R} = \begin{bmatrix} R_{11} & 0 & 0 \\ 0 & R_{11} & 0 \\ 0 & 0 & R_{33} \end{bmatrix}, \quad (6.105)$$

where we have set  $R_{22} = R_{11}$  for reasons of symmetry. The conditions for optimum (6.90) and for maximum power (6.95) give

$$\mathbf{U} = \begin{bmatrix} \hat{F}_{e,1}/2R_{11} \\ \hat{F}_{e,2}/2R_{22} \\ \hat{F}_{e,3}/2R_{33} \end{bmatrix} \quad (6.106)$$

$$P_{\text{MAX}} = \frac{1}{4} \hat{\mathbf{F}}_e^T \mathbf{U}^* = \frac{1}{8} \left( \frac{|f_1|^2}{R_{11}} + \frac{|f_2|^2}{R_{22}} + \frac{|f_3|^2}{R_{33}} \right) |A|^2. \quad (6.107)$$

From Eqs. (5.285) and (5.289), we have

$$f_1(\beta) = -f_{10} \cos \beta \quad (6.108)$$

$$f_2(\beta) = -f_{20} \sin \beta \quad (6.109)$$

$$f_3(\beta) = f_{30}, \quad (6.110)$$

and by using Eq. (5.302), we finally arrive at

$$\begin{aligned} P_{\text{MAX}} &= \frac{1}{8} \frac{4\rho g^2 D(kh)}{\omega k} \left( \cos^2 \beta + \sin^2 \beta + \frac{1}{2} \right) |A|^2 \\ &= \frac{3}{k} \frac{\rho g^2 D(kh)}{4\omega} |A|^2 = \frac{3}{k} J. \end{aligned} \quad (6.111)$$

The maximum absorption width is

$$d_{a,\text{MAX}} = \frac{P_{\text{MAX}}}{J} = \frac{3}{k} = \frac{3}{2\pi} \lambda. \quad (6.112)$$

This result was first obtained by Newman [34].

For the case with oscillation in just the three modes—surge, heave and pitch—the radiation resistance matrix is singular. (It is a  $3 \times 3$  matrix of rank 2.) As shown in Problem 6.3, the result is again and  $d_{a,\text{MAX}} = 3/k = (3/2\pi)\lambda$ .

Let us now consider the more general case in which all six modes of motion are allowed. The maximum power as given by Eq. (6.111) corresponds to optimum interference of the incident wave with three radiated circular waves, which have three possible different  $\theta$  variations, in accordance with Eq. (5.285). So, for instance, if surge is already involved and optimised, it is not possible to improve the optimum situation by also involving pitch, since both these modes produce radiated waves with the same  $\theta$  variation. If three modes of motion corresponding to three different  $\theta$  variations [see Eq. (5.285)] are already involved with their complex amplitudes chosen to yield optimum wave interference between the three radiated circular waves and the plane incident wave, then it is not possible to increase the absorbed power by increasing the number of degrees of freedom beyond three. Hence, the rank of the radiation resistance matrix for an axisymmetric system, as given by Eq. (5.302), cannot be more than three. Thus, the matrix is necessarily singular if its dimension is larger than  $3 \times 3$ .

## Problems

### Problem 6.1: Power Absorbed by a Heaving Buoy

An axisymmetric buoy has a cylindrical part, of height  $2l = 8$  m and of diameter  $2a = 6$  m, above a hemispherical lower end. The buoy is arranged to have a draught of  $l + a = 7$  m in its equilibrium position. The heave amplitude  $|\hat{s}|$  should be limited to  $l$ . Assume that this power buoy is equipped with a machinery by which the oscillatory motion can be controlled. Firstly, the heave speed is controlled to be in phase with the heave excitation force. Secondly, the damping of the oscillation should be adjusted for (optimum amplitude corresponding to) maximum absorbed power with small waves and for necessary limitation of the heave amplitude in larger waves. Apart from the amplitude limitation, we shall assume that linear theory is applicable. Moreover, we shall assume that the wave, as well as the heave oscillation, is sinusoidal. Deep water is assumed. The density of sea water is  $\rho = 1020$  kg/m<sup>3</sup>, and the acceleration of gravity  $g = 9.81$  m/s<sup>2</sup>.

- Using numerical results from Problem 5.12, calculate and draw graphs for the absorbed power  $P$  as function of the amplitude  $|A|$  of the incident wave when the wave period  $T$  is 6.3 s, 9.0 s, 11.0 s and 15.5 s. For each period, it is necessary to determine the wave amplitude  $|A_c|$  above which the design limit of the heave amplitude comes into play.
- Let us next assume that the average absorbed power has to be limited to  $P_{\max} = 300$  kW due to the design capacity of the installed machinery. For this reason, it is desirable (as an alternative to completely stopping the heave oscillation) to adjust the phase angle  $\gamma$  between the velocity and the excitation force to a certain value ( $\gamma \neq 0$ ) such that the absorbed power becomes  $P_{\max}$ . For this situation of very large incident wave, calculate and

draw a graph for  $\gamma$  as a function of  $|A|$  for each of the four mentioned wave periods.

- (c) Discuss (verbally) how this will be modified if we, instead of specifying  $P_{\max} = 300 \text{ kW}$  for the machinery, specify a maximum external damping force amplitude  $|F_u|_{\max} = 2.4 \times 10^5 \text{ N}$  or
- (d) a maximum load resistance  $R_u = 1.0 \times 10^5 \text{ N s m}^{-1}$ .

### Problem 6.2: Ratio of Absorbed Power to Volume

Assume that an incident regular (sinusoidal) wave of amplitude  $|A| = 1 \text{ m}$  is given (on deep water). Consider wave periods in the interval  $5 \text{ s} < T < 16 \text{ s}$ . A heaving buoy is optimally controlled for maximum absorption of wave energy (cf. Problem 6.1). The buoy is shaped as a cylinder with a hemispherical bottom, and it has a diameter of  $2a$  and a total height of  $a + 2l$ , where  $2l$  is the height of the cylindrical part. The equilibrium draught is  $a + l$ . Apart from the design limit  $l$  for the heave amplitude, we shall assume that linear theory is valid.

- (a) Derive an expression for the ratio  $P/V$  between the absorbed power  $P$  and the volume  $V$  of the buoy, in terms of  $\rho$ ,  $g$ ,  $a$ ,  $l$ ,  $|A|$ ,  $\omega = 2\pi/T$ ,  $|f_3|/S$  and  $\omega R_{33}/S$ . (See Problem 5.12 for a definition of some of these symbols.) With a fixed value for  $l$ , show that  $P/V$  has its largest value when  $a \rightarrow 0$ . Draw a curve for  $(P/V)_{\max}$  versus  $T$ .
- (b) Using results from Problem 6.1, draw a curve for  $P/V$  versus  $T$ , when  $a = 3 \text{ m}$  and  $l = 4 \text{ m}$ . In addition to the scale for  $P/V$  (in  $\text{kW/m}^3$ ), include a scale for  $P$  (in  $\text{kW}$ ). Also draw a curve for how  $P$  would have been if there had been no limitation of the heave amplitude.

### Problem 6.3: Maximum Absorbed Power by an Axisymmetric Body

The maximum power absorbed by an oscillating body in a plane incident wave is

$$P_{\max} = \frac{1}{2} \mathbf{U}^T \mathbf{R} \mathbf{U}^*,$$

where  $\mathbf{R}$  is the radiation resistance matrix and where the optimum velocity vector  $\mathbf{U}$  has to satisfy the algebraic equation

$$\mathbf{R} \mathbf{U} = \hat{\mathbf{F}}_e / 2,$$

where  $\hat{\mathbf{F}}_e$  is a vector composed of all (six) excitation force components of the body. Let  $\lambda$  denote the wavelength and  $J$  the wave power transport of the incident plane harmonic wave.

Use the reciprocity relation between the radiation resistance matrix and the excitation force vector to show that an axisymmetric body oscillating with optimum complex amplitudes absorbs a power

- (a)  $P_{\text{MAX}} = (3\lambda/2\pi)J$  if it oscillates in the surge and heave modes only,
- (b)  $P_{\text{MAX}} = (\lambda/\pi)J$  if it oscillates in the surge and pitch modes only and
- (c)  $P_{\text{MAX}} = (3\lambda/2\pi)J$  if it oscillates in the surge, heave and pitch modes only.

State the conditions which the optimum complex velocity amplitudes have to satisfy in each of the three cases, (a)–(c). It is assumed that linear theory is applicable; that is, the wave amplitude is sufficiently small to ensure that the oscillation amplitudes are not restricted.

#### Problem 6.4: Alternative Derivation of the Wave-Power ‘Island’

Let us define  $U_0 = \hat{F}_e/\sqrt{8R_{jj}}$  and  $U = \hat{u}_j\sqrt{R_{jj}/2}$ . Then, on the basis of Eqs. (6.4)–(6.6) and (6.12), show that

$$P_{\text{MAX}} - P = |U_0 - U|^2.$$

#### Problem 6.5: Maximum Absorbed Power with Optimised Amplitude

The maximum absorbed power when the amplitude but not the phase of the oscillation is optimised is, for two different situations, given by Eqs. (3.41) and (6.10). In the former case, the oscillation is restricted by the dynamic equation (3.30), whereas in the latter case, the oscillation amplitude is chosen at will (which may necessitate that a control device is part of the system).

- (a) For the situation to which Eq. (3.41) pertains, determine the phase angle  $\gamma$  between the velocity and the excitation force, in terms of  $x \equiv (\omega m_m + \omega m_r - S/\omega)/R_r$ , and express  $P_{a,\text{max}}$  in terms of  $\hat{F}_e$ ,  $R_r$  and  $x$ .
- (b) Setting  $\gamma_j = \gamma$ ,  $R_{jj} = R_r$  and  $\hat{F}_{ej} = \hat{F}_e$ , apply Eq. (6.10) to express  $P_{\text{max}}$  in terms of  $\hat{F}_e$ ,  $R_r$  and  $x$ .
- (c) Then express  $p \equiv P_{\text{max}}/P_{a,\text{max}}$  in terms of  $x$ , and show that  $p \geq 1$ . Finally, show that  $p = 1$  for resonance ( $x = 0$ ).